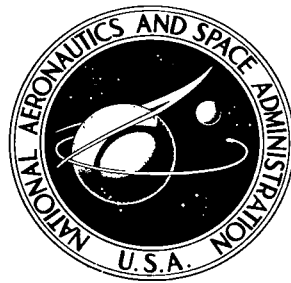


NASA TECHNICAL NOTE



NASA TN D-4541

C.1

NASA TN D-4541



LOAN COPY: RET.
AFWL (WLIL-2)
KIRTLAND AFB, N MEX

CRACK GROWTH IN 2014-T6 ALUMINUM TENSILE
AND TANK SPECIMENS CYCLICALLY LOADED
AT CRYOGENIC TEMPERATURES

by William S. Pierce
Lewis Research Center
Cleveland, Ohio



CRACK GROWTH IN 2014-T6 ALUMINUM TENSILE AND TANK SPECIMENS
CYCLICALLY LOADED AT CRYOGENIC TEMPERATURES

By William S. Pierce

Lewis Research Center
Cleveland, Ohio

NATIONAL AERONAUTICS AND SPACE ADMINISTRATION

For sale by the Clearinghouse for Federal Scientific and Technical Information
Springfield, Virginia 22151 - CFSTI price \$3.00

CRACK GROWTH IN 2014-T6 ALUMINUM TENSILE AND TANK SPECIMENS CYCLICALLY LOADED AT CRYOGENIC TEMPERATURES

by William S. Pierce

Lewis Research Center

SUMMARY

An investigation was conducted to determine the cryogenic low-cycle (life under 1000 cycles) fatigue crack growth behavior of 2014-T6 aluminum through-notched uniaxial tensile and biaxial pressure vessel specimens. The specimen thickness was 0.060 inch (0.15 cm). Low-cycle crack growth data were obtained from the notched specimens at -320° and -423° F (77° and 20° K). Initial notch lengths from 0.125 to 1.0 inch (0.318 to 2.54 cm) and initial R ratios R_i (minimum to maximum initial stress intensity factor, $K_{\min, i}/K_{\max, i}$) from 0.07 to 0.36 were studied.

The parameters R_i and $K_{\max, i}$ appear to be useful for relating crack growth rates in pressure vessels to those in tensile specimens. At -320° and -423° F (77° and 20° K), the crack growth rates were almost equal for the pressure vessel and corresponding tensile specimen provided the R_i and $K_{\max, i}$ values were held constant.

The slopes of the curves for crack growth rate da/dN as a function of stress intensity factor range ΔK varied from 6 to 13 on a log-log plot. This slope is a function of R_i and increases as R_i increases. The values obtained for the slopes were, in general, higher than those in the literature for similar tests conducted at room temperature.

For a given ratio of maximum to critical stress intensity factor, the specimens tested at -423° F (20° K) had longer lives than those tested at -320° F (77° K). Also, specimens run with higher R_i ratios had the longer cyclic lives for a given ratio of maximum to critical stress intensity. For similar values of R_i and $K_{\max, i}$, the cyclic lives of tensile and tank specimens were almost equal, with the tensile specimens generally having longer lives.

INTRODUCTION

Cryogenic propellant tanks for advanced space missions may be subjected to many

cycles of pressurization and external loading during the test, launch, and flight phases. There may be, therefore, an opportunity for flaws, which were not critical initially, to grow due to cyclic loading to either the leak or burst stage. Such flaws may be present in the parent material or may result from the fabrication processes. Also, some flaws may be added during flight in the form of micrometeoroid damage. Depending on the severity of the damage and the material characteristics, the results can be immediately catastrophic. More likely, however, the damage is of a form that provides an initiation site for flaw growth under sustained load or additional cyclic loading.

To assist in assuring the required reliability, it is necessary to develop a proof testing program for each propellant tank. The loads and pressures applied during the proof test must be of levels that assure the absence of any flaws large enough to grow to a critical size during the required vehicle life. The development of a proof testing program requires knowledge of flaw propagation rates in the material under the appropriate loading and environmental conditions. To obtain the necessary data from pressure vessel type specimens is difficult and expensive. It is highly desirable, therefore, to gather the required data from tests of flawed uniaxial specimens. There are questions, however, that arise in translating the uniaxial flaw growth data into actual tank flaw growth and ultimate failure.

In recent years considerable effort has been expended in studies of flaw growth characteristics under conditions leading to low-cycle fatigue. For example, Paris (ref. 1) developed a thin-sheet flaw growth relation for uniaxial specimens at room temperature. Tiffany, Lorenz, and Hall (ref. 2) developed design criteria for plane strain flaw growth in tanks and uniaxial specimens at room and cryogenic temperatures. At the same time, Eitman and Rawe (ref. 3) developed parametric relations for thin-sheet flaw growth in tank and uniaxial specimens of 2219-T87 aluminum alloy at cryogenic temperatures.

Research was conducted at the Lewis Research Center to establish a correlation of flaw growth between uniaxially and biaxially stressed sheet specimens subjected to cyclic loading at cryogenic temperatures in terms of fracture mechanics concepts. A secondary objective of this research was to determine the effect of initial R ratio R_i (minimum to maximum initial stress intensity ratio, $K_{\min, i}/K_{\max, i}$) on the flaw growth relation. In addition, it was desired to explore the low-cycle flaw growth process in a cycle range commensurate with the number of cycles of loading that an advanced propellant tank or pressurization bottle might be expected to undergo during its life. This range was therefore selected to be from 0 to 1000 cycles. The material chosen for this investigation was the aluminum alloy 2014-T6, which is currently being used in several vehicle systems.

Flaws extending through the thickness of the sheet material were chosen for the initial investigation as a first step in the overall program. This was done because of simplifications involved in both the experimental and theoretical approaches to the problem.

It is recognized, however, that flaws extending partially through the thickness are probably of more concern from a practical point of view and subsequent phases of the overall program will be concerned with this type.

This report presents the results of tests to determine the flaw growth characteristics of through cracks in uniaxially and biaxially loaded specimens of 2014-T6 aluminum sheet at -320° and -423° F (77° and 20° K) resulting from cyclic loading in the 0 to 1000 cycle range. A correlation is presented in terms of fracture mechanics relations and the effect of R_1 ratio on the flaw growth and cyclic life is shown.

SYMBOLS

2a	crack length, in.; cm
C	dimensionless bulge coefficient (eq. (2))
C*	constant in crack propagation equation accounting for mean load, loading frequency and environment (eq. (3))
C_1, C_2	constants in crack propagation equations accounting for material and environment (eqs. (4) and (5))
K	stress intensity factor, ksi $\sqrt{\text{in.}}$; MN/m $^{3/2}$
ΔK	stress intensity factor range, $K_{\text{max}} - K_{\text{min}}$, ksi $\sqrt{\text{in.}}$; MN/m $^{3/2}$
N	load cycles
n	exponent in crack propagation equation (eq. (4))
R	ratio of $K_{\text{min}}/K_{\text{max}}$ in a given cycle
r	radius of tank, in.; cm
w	sheet width, in.; cm
γ	slope on a log-log plot of da/dN against ΔK
σ	uniform gross stress acting normal to plane of crack, psi; MN/m 2
$\Delta \sigma$	stress range ($\sigma_{\text{max}} - \sigma_{\text{min}}$), psi; MN/m 2
σ_y	uniaxial yield strength, psi; MN/m 2
σ_{yB}	yield strength in 2:1 stress field, psi; MN/m 2

Subscripts:

c	critical
F	failure

H	hoop direction in cylindrical tank
i	initial condition (start of test)
L	last complete cycle
max	value at maximum cyclic load
min	value at minimum cyclic load

MATERIAL, APPARATUS, AND PROCEDURES

Material and Specimens

The material used in this investigation was from a single heat of unclad 2014-T6 extruded aluminum alloy tubing. The chemical analysis of this heat is given in table I.

The tensile specimens were machined from the same tubing as the tank specimens. Pieces of tubing were cut longitudinally, annealed, flattened, and reheat-treated to the T6 condition. Hardness tests were performed as a check for the T6 condition. Specimens were machined from the flattened tubes to the shape shown in figure 1. All specimens were transverse with respect to the extruding direction. A finished notched specimen with continuity gages is shown in figure 2.

The tank specimens were machined from the 6 inch (15.2 cm) outside diameter by 0.25 inch (0.63 cm) wall extruded tubing. The finished wall thickness was $0.060^{+0.002}_{-0.000}$ inch ($0.152^{+0.005}_{-0.000}$ cm) with a mean diameter of 5.63 inches (14.3 cm). Longitudinal notches were machined in the tanks and were shaped as shown in figure 1. A finished specimen with special ends, strain gages, and continuity gages is shown in figure 3.

The actual dimensions for each specimen were used in the calculations and data presented. The tolerances are given to show the range of a particular dimension. Machined notches were used instead of fatigue tipped for two primary reasons:

(1) Previously unpublished data by the author indicated practically no difference between failure stresses for machine notched (0.0002 in., 0.0005 cm, radius) and fatigue-tipped-notched tanks in this material and thickness.

(2) Because the specimens exhibited crack growth on the first cycle, no initiation time was involved.

Once crack growth occurs, the original notch should have little, if any, effect on the growth process, provided the notching process does not affect adjacent material.

Apparatus

Static tensile tests. - A tensile machine with a hydraulically actuated loading frame was used for the tensile tests. A vacuum-jacketed cryostat was used to contain the cryogenic fluid that surrounded the test specimen. Strain was measured by using a clamp-on differential-transformer extensometer with a 2-inch (5-cm) gage length and an autographic stress-strain recorder.

Static tank tests. - In references 4 and 5 a complete description is given of the method used for bursting tanks at -320° and -423° F (77° and 20° K). The system is capable of bursting tanks at pressures up to 3000 psi (20.7×10^6 N/m²).

Cyclic tensile tests. - The tensile fatigue testing machine is shown in figure 4. It consists of a load frame and cryostat. A hydraulic piston is located on top of the load frame and loads through a load cell at the top. In the figure the cryostat is lowered to show the position of the test specimen; during testing the cryostat is raised to surround the test specimen. The machine uses a servo-controller in conjunction with a function generator to control the load history. Load capacity is 20 000 pounds (89 000 N), and the cyclic rate used was 3 cycles per minute (0.05 Hz).

Cyclic tank tests. - The test cell, cryostat, and special tank end closures are described in references 4 and 5. For the -320° F (77° K) cyclic tank tests, gaseous nitrogen was used as the pressurizing medium instead of gaseous helium as outlined in reference 4. Cycling was accomplished by alternately pressurizing and venting the gaseous nitrogen. Pressure controlled valves were used to control the flow of gaseous nitrogen. Cycle rate was 3 cycles per minute (0.05 Hz).

The tank tests at -423° F (20° K) were similar to the -320° F (77° K) test except that liquid hydrogen was used for pressurization. A 2.5-gallon-per-minute (9.4×10^{-3} m³/min) liquid-hydrogen pump capable of 4000 psi (27.6×10^6 N/m²) was used to pressurize the test tank. The rate was 3 cycles per minute (0.05 Hz).

Instrumentation. - Carbon resistor probes were used to determine the liquid level in the cryostats. In all tests, however, the test specimen was submerged in the appropriate cryogenic liquid.

Crack length was measured by use of foil element continuity gages. A complete description of the gage and its use is found in reference 6. The cyclic calibration is described in that reference. Figure 5 shows two continuity gages mounted in tandem at the notch tip.

Procedure

Static tensile tests. - Tensile tests to determine the ultimate strength and

0.2-percent-offset yield strength were run at approximately 70° F (293° K) in ambient air, -320° F (77° K) in liquid nitrogen, and -423° F (20° K) in liquid hydrogen. Specimens with a 1.0-inch (2.54-cm) notch length were tested at -320° and -423° F (77° and 20° K) to determine the apparent fracture toughness value (K_{Ic}) for the extruded material when machined to a thickness of 0.060 inch (0.15 cm). The notch length used for the fracture toughness calculations was the critical notch length obtained when the crack propagation velocity approached 0.5 to 1.0 inch (1.3 to 2.5 cm) per second (ref. 7). The validity of this specimen size is also shown in reference 7. A minimum of two specimens was run for each test condition. Average values of these data are listed in table II.

Static tank tests. - One unnotched tank was tested at -320° and -423° F (77° and 20° K) to determine the biaxial 0.2-percent-offset yield strength. Foil strain gages were used to measure the strain in the tank wall. The mounting technique and gage type are described in reference 8.

Cyclic tensile tests. - Axial-tension fatigue tests were conducted on tensile specimens with initial notch lengths $2a_i$ equal to approximately 0.125, 0.300, 0.500, and 1.000 inch (0.318, 0.762, 1.27, and 2.54 cm). The specimen width was 3.00 inches (7.6 cm). At -320° F (77° K) approximately four specimens were tested at each notch length (see table III). The maximum cyclic stress level for each of the four specimens was chosen to give various cyclic lives up to approximately 1000 cycles. The minimum cyclic stress was fixed at 4.6 ksi (31.7×10^6 N/m²) due to limitations of the test equipment in the early stages of the program. Due to the fixed minimum stress and varied maximum stress, the R_i ratio varied from approximately 0.07 to 0.23. The cyclic rate was 3 cycles per minute (0.05 Hz).

At -423° F (20° K) similar tests were run but with only one specimen at each notch length because the results were very similar to the -320° F (77° K) data. For these tests the minimum cyclic stress was varied to give particular values for R_i (see tensile data, table IV).

Cyclic tank tests. - Biaxial fatigue tests were conducted on tanks for the same notch lengths and test temperatures as the tensile fatigue tests. The tanks were immersed in and filled with the cryogenic liquid. To have a common factor between the tank and tensile tests, the initial maximum stress intensity factor ($K_{max, i}$) was held equal for a particular tank and corresponding tensile specimen (see BASIS OF DATA ANALYSIS section). The minimum cyclic stress was again held at 4.6 ksi (31.7×10^6 N/m²) (see tank data, tables III and IV). The cycle rate was approximately 3 cycles per minute (0.05 Hz).

BASIS OF DATA ANALYSIS

The Irwin equation (ref. 9) with plastic zone correction was used for calculation of

stress intensity factors K of the tensile specimens. The equation has the form

$$K = \sigma \sqrt{w \tan \left[\frac{\pi}{w} \left(a + \frac{1}{2\pi} \frac{K^2}{\sigma_y^2} \right) \right]} \quad (1)$$

An equation recently developed by M. Isida has been shown to be more accurate than the Irwin tangent equation when the aspect ratio ($2a/w$) is greater than 0.1 (ref. 10). Therefore equation (1) results in K values that are a maximum of 9 percent low when the final notch length ($2a_L$) was 2.0 inches (5.1 cm), aspect rates equal to 0.67. For most of the test results this error is much less.

For the tank specimens the equation with bulge correction developed by Anderson (ref. 11) was used to determine K . This equation takes the form

$$K = \sigma_H \sqrt{\pi a + \frac{1}{2} \frac{K^2}{\sigma_{yB}^2} \left(1 + \frac{Ca}{r} \right)} \quad (2)$$

As described in the Procedure section (p. 5), the maximum cyclic tensile stresses were chosen to give a range of values for cyclic life. Also, the initial maximum stress intensity factors ($K_{\max, i}$) were to be equal for a tensile specimen and the corresponding tank specimen. Therefore, to calculate the maximum cyclic hoop stress $\sigma_{H_{\max}}$ for the tank specimens, the procedure was as follows:

(1) The initial maximum stress intensity factor $K_{\max, i}$ was calculated for the tensile specimens by using equation (1), the initial tensile specimen geometry, maximum cyclic stress, and the tensile yield strength.

(2) Substituting the value of $K_{\max, i}$ into equation (2) along with the tank specimen geometry, biaxial yield strength, and a value for C from reference 11 gives the required maximum cyclic hoop stress $\sigma_{H_{\max}}$.

Figure 6 is typical of the curves obtained for crack growth as a function of stress cycles. Data were plotted and a smooth curve drawn to give a good visual fit. Ten points were selected on each curve. At each point the slope $d(2a)/dN$ was determined graphically and K_{\max} and K_{\min} were calculated using either equation (1) for tensile or equation (2) for tank specimens (tables V, VI, and VII). The crack growth rate da/dN as a function of stress intensity factor range ΔK is plotted in figures 7(a) to (r). The slope γ was determined using a least-square best-fit computer program.

RESULTS AND DISCUSSION

Tank and Tensile Correlation

Figures 7(a) to (r) show the crack growth rate da/dN as a function of crack tip stress intensity factor range ΔK and the calculated slope γ for tank and tensile specimens. The R_i ratio ($K_{min,i}/K_{max,i}$) varies from 0.068 to 0.355. Figures 7(a) to (n) are for -320° F (77° K); figures 7(o) to (r) are for -423° F (20° K). For tests in which the values of $K_{max,i}$ and R_i were approximately equal for the tensile and tank specimens, the tank and tensile data are in fairly close agreement. In figures 7(l) to (n), the values of $K_{max,i}$ were the same for tank and tensile tests, but the R_i value was considerably different, and the two sets of data are more widely separated. Therefore, it appears that when R_i and $K_{max,i}$ are the same for tank and tensile specimens, the crack growth rates da/dN are almost equal for a given stress intensity range ΔK . Similar results were obtained for tests run at -423° F (20° K), figures 7(o) to (r).

In figures 7(e), (f), (i), and (l) the curves of da/dN against ΔK are initially somewhat flat or have a negative slope. These curves are for the tests that had the highest $K_{max,i}$. The flatness or negative slope may be the result of notch blunting or high compressive stresses at the crack tip created during the first cycle; as a result, the crack growth rate was initially reduced. These few points were not included in the least-square curve fit.

Crack Growth Laws and R Ratio

The crack propagation law proposed by Paris (ref. 1)

$$\frac{da}{dN} = C * \Delta K^\gamma \quad (3)$$

(where $\gamma = 4$) gives good results for moderate- to high-cycle life test conditions. However, it does not appear to adequately account for the effect of R ratio changes on crack growth rate in the low-cycle region as observed in this study. Figure 8 was compiled from figures 7(a) to (r) and shows the effect of R_i ratio on the slope γ of the da/dN against ΔK plots. The value for γ ranged from 6 to 13. These values are much higher than the value of 4 proposed by Paris. However, it should be pointed out that the data from which Paris proposed his fourth-power relation were for N_F in the range of 10^4 to 10^6 cycles. This is indicative of $K_{max,i}$ being at a fairly low percentage of K_C . The

data reported here are for cyclic lives primarily less than 1000 cycles and $K_{\max, i}$ above $0.4 K_c$.

Carman and Katlin (ref. 12) point out that for their data the fourth-power relation held until the value of K reached 0.7 to 0.8 of K_c , then a greatly accelerated growth rate occurred. Clark (ref. 13) shows values of $\gamma = 9$ for some high-strength steels under plane strain conditions. In reference 14, Hudson applied several crack growth laws to data with various R ratios at room temperature and found that a relation developed by Forman, Kearny, and Engle (ref. 15) best fit the data. That equation is

$$\frac{da}{dN} = \frac{C_1 (\Delta K)^n}{(1 - R)K_c - \Delta K} \quad (4)$$

This equation was applied to part of the data in this study with some success. However, at higher values of R_i , the predicted growth rates were still quite low (up to a factor of 10) with respect to the data. Therefore, it appears that for data in the low-cycle region, a crack growth law might take a form such as

$$\frac{da}{dN} = C_2 \Delta K^\gamma \quad (5)$$

where γ is a function of R_i ratio and C_2 is a constant depending on material and environment.

Effect of R Ratio on Crack Growth

In figure 8 as the R_i ratio is increased the slope γ generally increased. Therefore, referring to figures 7(a) to (r), an increase in R_i means an increase in γ and an increase in crack growth rate da/dN for a given value of ΔK . This is true for specimens tested at both -320° and -423° F (77° and 20° K). It should be pointed out that since R equals $1 - (\Delta K/K_{\max})$ or (K_{\min}/K_{\max}) , to increase the R ratio and hold ΔK constant requires an increase in both K_{\min} and K_{\max} .

Effect of Stress Intensity on Cycles to Failure

Figures 9(a) and (b) show the effect of $K_{\max, i}/K_c$ and R_i ratio on cycles to failure for tensile and tank specimens, respectively. Tests with higher values of R_i have

longer lives at a given percent of critical; correspondingly, tests run at -423° F (20° K) had longer lives than those run at -320° F (77° K).

For similar initial conditions for R ratio and K_{\max} , the cyclic lives of tensile and tank specimens were almost equal, with the tensile specimens generally having longer lives.

SUMMARY OF RESULTS

An investigation was conducted to determine the cryogenic low-cycle fatigue crack growth behavior and cyclic life of 2014-T6 aluminum through notched tank and tensile specimens. Low-cycle crack growth data were obtained from the notched specimens in liquid nitrogen and liquid hydrogen. Various notch lengths and R_i ratios (minimum to maximum initial stress intensity factors, $K_{\min, i}/K_{\max, i}$) were studied. The following results were obtained:

1. The R_i ratio appears to be a useful parameter for relating crack growth rate in tensile specimens to the crack growth rate in tanks. When the R_i ratio and the initial maximum stress intensity factor $K_{\max, i}$ are the same for the tank and tensile specimens, the crack growth rates da/dN are essentially equal for a given stress intensity factor range ΔK . This is true for specimens run at both -320° F (77° K) and 20° K .
2. For the cyclic range studied (less than 1000 cycles and high $K_{\max, i}$), the relation for crack growth might take a form such as $(da/dN) = C_2 \Delta K^{\gamma}$, where the slope γ is a function of the R_i ratio and C_2 is a constant accounting for material and environment. The values for γ ranged from 6 to 13. These values are much higher than the value of 4.0 that Paris obtained; however, Paris' data were for the 10^4 to 10^6 cycle region. Similar results were obtained for both test temperatures.
3. When the stress intensity factor range ΔK is held constant, the rate of crack growth generally increases with increasing R_i ratio. This is true for tests run at both -320° F (77° K) and -423° F (20° K).
4. The curves of $K_{\max, i}/K_c$ against the cycles to failure N_F shows that specimens tested at higher R_i ratios have longer lives than those tested at lower R_i ratios; correspondingly, specimens run at -423° F (20° K) had longer lives than those run at -320° F (77° K). Also, for similar initial conditions, the cyclic lives of tensile and tank specimens were almost equal, with the tensile specimens generally having longer lives.

Lewis Research Center,

National Aeronautics and Space Administration,

Cleveland, Ohio, December 18, 1967,

124-08-08-20-22.

REFERENCES

1. Paris, Paul C.: The Growth of Cracks Due to Variations in Load. PhD Thesis, Lehigh University, 1962.
2. Tiffany, C. F.; Lorenz, P. M.; and Hall, L. R.: Investigation of Plane-Strain Flaw Growth in Thick-Walled Tanks. Rep. No. D2-24078-1 (NASA CR-54837), Boeing Company, Feb. 1966.
3. Eitman, D. A.; and Rawe, R. A.: Plane Stress Cyclic Flaw Growth of 2219-T87 Aluminum and 5Al-2.5 Sn ELI Titanium Alloys at Room and Cryogenic Temperatures. Rep. No. DAC-59256 (NASA CR-54956), Douglas Aircraft Co., Sept. 1, 1966.
4. Calvert, Howard F.; and Kemp, Richard H.: Determination of Pressure Vessel Strengths at -423° F as Influenced by Notches of Various Radii. Paper No. 520B, SAE, Apr. 1962.
5. Getz, David L.; Pierce, William S.; and Calvert, Howard F.: Correlation of Uniaxial Notch Tensile Data with Pressure-Vessel Fracture Characteristics. Paper No. 63-WA-187, ASME, Nov. 1963.
6. Sullivan, Timothy L.; and Orange, Thomas W.: Continuity Gage Measurement of Crack Growth on Flat and Curved Surfaces at Cryogenic Temperatures. NASA TN D-3747, 1966.
7. Orange, Thomas W.: Fracture Toughness of Wide 2014-T6 Aluminum Sheet at -320° F. NASA TN D-4017, 1967.
8. Kaufman, Albert: Performance of Electrical-Resistance Strain Gages at Cryogenic Temperatures. NASA TN D-1663, 1963.
9. Irwin, G. R.: Fracture Testing of High-Strength Sheet Materials Under Conditions Appropriate for Stress Analysis. Rep. No. 5486, Naval Research Lab., July 27, 1960.
10. Brown, William F., Jr.; and Srawley, John E.: Plane Strain Crack Toughness Testing of High Strength Metallic Materials. ASTM STP 410, 1967.
11. Anderson, Robert B.; and Sullivan, Timothy L.: Fracture Mechanics of Through-Cracked Cylindrical Pressure Vessels. NASA TN D-3252, 1966.
12. Carman, C. M.; and Katlin, J. M.: Low Cycle Fatigue Crack Propagation Characteristics of High Strength Steels. J. Basic Eng., vol. 88, no. 4, Dec. 1966, pp. 792-800.

13. Clark, W. G., Jr.: Subcritical Crack Growth and Its Effect Upon the Fatigue Characteristics of Structural Alloys. Paper No. 67-1D6-BTLFR-P1, Research and Dev. Center, Westinghouse Research Lab., Feb. 1967.
14. Hudson, C. M.; and Scardina, J. T.: Effect of Stress Ratio on Fatigue-Crack Growth in 7075-T6 Aluminum-Alloy Sheet. Paper presented at the National Symposium on Fracture Mechanics, Bethlehem, Pa., June 19-21, 1967.
15. Forman, R. G.; Kearney, V. E.; and Engle, R. M.: Numerical Analysis of Crack Propagation in Cyclic-Loaded Structures. J. Basic Eng., vol. 89, no. 3, Sept. 1967, pp. 459-464.

TABLE I. - CHEMICAL ANALYSIS OF TEST MATERIAL

Composition, wt %									
Cu	Fe	Si	Mn	Mg	Zn	Ni	Cr	Ti	Sn
4.32	0.35	0.80	0.73	0.40	0.06	0.005	0.01	0.025	0.001

TABLE II. - MECHANICAL PROPERTIES OF 2014-T6 ALUMINUM ALLOY^a

	Ambient air (70° F; 293° K)	Liquid nitrogen (-320° F; 77° K)	Liquid hydrogen (-423° F; 20° K)
Uniaxial yield strength, ksi (MN/m ²)	63.3 (440)	75.0 (520)	81.6 (560)
Biaxial yield strength, ksi (MN/m ²)	-----	85.8 (590)	93.8 (650)
Ultimate tensile strength, ksi (MN/m ²)	75.0 (520)	86.0 (590)	99.7 (690)
Fracture toughness, K _{IC} , ksi√in. (MN/m ^{3/2})	-----	64.6 (71)	55.1 (61)

^aSpecimen thickness, 0.060 in. (0.15 cm).

TABLE III. - INITIAL CONDITIONS AND TEST DATA AT -320°F (77°K)

(a) U.S. customary units

Symbol	Specimen number	$2a_i$, in.	$2a_{L'}$, in.	σ_{\min} , ksi	σ_{\max} , ksi	$\Delta\sigma$, ksi	σ_F , ksi	N_F , cycles to failure	$K_{\min, i}$, ksi $\sqrt{\text{in.}}$	$K_{\max, i}$, ksi $\sqrt{\text{in.}}$	ΔK_i , ksi $\sqrt{\text{in.}}$	$\Delta K_i/K_c$	$K_{\max, i}/K_c$	R_i	$\Delta K_i/K_{\max, i}$	$K_{\max, L'}$, ksi $\sqrt{\text{in.}}$	γ
Tensile																	
○	1	0.126	0.59	4.6	57.3	52.7	56.2	215	2.1	30.4	28.3	0.44	0.47	0.068	0.932	69.0	7.3
□	2	.126	.56		54.2	49.6	52.0	277	2.0	28.1	26.1	.40	.43	.073	.927	61.4	7.6
◇	3	.128	.84		52.5	47.9	50.7	751	2.1	27.1	25.1	.39	.42	.076	.924	76.1	6.7
△	4	.128	.94		47.8	43.2	46.1	1163	2.1	24.1	22.0	.34	.37	.086	.914	71.8	6.3
▴	5	.301	.74		47.6	43.0	46.3	70	3.2	36.9	33.7	.52	.57	.086	.914	60.7	9.8
▾	6	.300	.82		44.7	40.1	43.4	133		34.1	30.9	.48	.53	.093	.907	59.5	7.9
◻	7	.296	.92		40.4	35.8	39.0	293		30.0	26.8	.42	.46	.105	.895	56.4	7.7
◊	8	.300	1.00		37.6	33.0	37.4	560	↓	27.8	24.6	.38	.43	.114	.886	54.5	7.8
◈	9	.496	1.13		37.6	33.0	37.0	116	4.1	36.1	32.0	.50	.56	.114	.886	59.6	8.8
◑	10	.495	1.29		35.5	30.9	34.7	174	4.1	33.8	29.7	.46	.52	.122	.878	61.6	8.3
◒	11	.496	1.64		30.0	25.4	29.2	1447	4.1	28.0	23.9	.37	.43	.147	.853	63.2	6.5
◓	12	1.001	1.67		28.1	23.5	27.8	131	6.1	38.9	32.8	.51	.60	.156	.844	59.2	11.2
◔	13	.999	1.79		25.0	20.4	23.8	400	6.1	34.2	28.1	.44	.53	.177	.823	55.8	11.1
◕	14	.992	1.82		21.4	16.8	21.0	1088	6.0	28.8	22.8	.35	.45	.209	.791	47.2	8.9
▽	15	.995	2.17	↓	19.6	15.0	19.6	1906	6.0	26.3	20.0	.31	.41	.230	.770	57.1	7.9
Tank																	
●	16	0.125	0.50	4.6	54.9	50.3	----	180	2.2	30.0	27.8	0.43	0.46	0.073	0.927	79.3	6.0
■	17		.51		51.8	47.2	49.9	356		27.8	25.6	.40	.43	.079	.921	73.5	6.2
◆	18		.48		50.1	45.5	----	584	↓	26.7	24.5	.38	.41	.082	.918	66.7	5.6
▲	19	↓	.53		45.4	40.8	45.4	1176	↓	23.6	21.4	.33	.37	.093	.907	63.1	6.0
▴	20	.300	.59		41.2	36.6	40.5	59	3.7	36.5	32.8	.51	.57	.102	.898	61.2	7.1
▾	21	.300	.68		38.6	34.0	37.7	81		33.8	30.1	.47	.52	.111	.889	63.3	7.3
◻	22	.300	.61		34.8	30.2	34.4	191		30.1	26.3	.41	.47	.124	.876	51.0	7.2
◊	23	.300	.69		32.3	27.7	31.8	358	↓	27.7	23.9	.37	.43	.135	.865	51.7	9.6
◈	24	.500	.90		29.5	24.9	29.5	118	5.3	36.0	30.7	.48	.56	.148	.852	58.8	8.6
◑	25	.500	.91		27.7	23.1	27.7	246	5.3	33.6	28.2	.44	.52	.159	.841	55.1	8.7
◒	26	.500	1.00		23.4	18.8	22.9	983	5.3	27.9	22.6	.35	.43	.191	.809	49.7	7.0
◓	27	1.00	1.40		18.5	13.9	18.1	30	9.3	38.6	29.3	.45	.60	.241	.759	53.2	12.8
◔	28	1.00	----		14.0	9.4	14.0	492	9.3	28.8	19.5	.30	.45	.323	.677	----	9.9
◕	29	1.00	1.66	↓	12.8	8.2	12.8	1613	9.3	26.3	16.9	.26	.41	.355	.645	42.7	11.1

(b) SI units

Symbol	Specimen number	$2a_i$, cm	$2a_L$, cm	σ_{min} , MN/m ²	σ_{max} , MN/m ²	$\Delta\sigma$, MN/m ²	σ_F , MN/m ²	N_F , cycles to failure	$K_{min,i}$, MN/m ^{3/2}	$K_{max,i}$, MN/m ^{3/2}	ΔK_i , MN/m ^{3/2}	$\Delta K_i/K_c$	$K_{min,i}/K_c$	R_i	$\Delta K_i/K_{max,i}$	$K_{max,L}$, MN/m ^{3/2}	γ
Tensile																	
○	1	0.320	1.499	31.7	395	364	388	215	2.3	33.4	31.1	0.44	0.47	0.068	0.932	75.9	7.3
□	2	.320	1.422		374	342	359	277		30.9	28.7	.40	.43	.073	.927	67.5	7.6
◇	3	.325	2.134		362	331	350	751		29.8	27.6	.39	.42	.076	.924	83.7	6.7
△	4	.325	2.388		330	298	318	1163		26.5	24.2	.34	.37	.086	.914	79.0	6.3
▴	5	.764	1.880		328	297	319	70	3.5	40.6	37.1	.52	.57	.086	.914	66.8	9.8
▾	6	.762	2.083		308	277	299	133		37.5	34.0	.48	.53	.093	.907	65.4	7.9
◻	7	.752	2.337		279	247	269	293		33.0	29.5	.42	.46	.105	.895	62.0	7.7
◇	8	.762	2.540		259	228	258	560		30.6	27.1	.38	.43	.114	.886	60.0	7.8
◊	9	1.260	2.870		259	228	255	116	4.5	39.7	35.2	.50	.56	.114	.886	65.6	8.8
▵	10	1.257	3.277		245	213	239	174	4.5	37.2	32.7	.46	.52	.122	.878	67.8	8.3
◻	11	1.260	4.166		207	175	201	1447	4.5	30.8	26.3	.37	.43	.147	.853	69.5	6.5
▾	12	2.543	4.242		194	162	192	131	6.7	42.8	36.1	.51	.60	.156	.844	65.1	11.2
▴	13	2.537	4.547		172	141	164	400	6.7	37.6	30.9	.44	.53	.177	.823	61.4	11.1
◇	14	2.520	4.623		148	116	145	1088	6.6	31.7	25.1	.35	.45	.209	.791	51.9	8.9
▽	15	2.527	5.512		135	104	135	1906	6.6	28.9	22.0	.31	.41	.230	.770	62.8	7.9
Tank																	
●	16	0.318	1.270	31.7	379	347	-----	180	2.4	33.0	30.6	0.43	0.46	0.073	0.927	87.2	6.0
■	17		1.295		357	326	344	356		30.6	28.2	.40	.43	.079	.921	80.8	6.2
●	18		1.219		346	314	-----	584		29.4	27.0	.38	.41	.082	.918	73.4	5.6
▲	19		1.346		313	282	313	1176		26.0	23.5	.33	.37	.093	.907	69.4	6.0
▴	20	.762	1.499		284	253	279	59	4.1	40.2	36.1	.51	.57	.102	.898	67.3	7.1
▾	21	.762	1.727		266	235	260	81		37.2	33.1	.47	.52	.111	.889	69.6	7.3
◻	22	.762	1.549		240	208	237	191		33.1	28.9	.41	.47	.124	.876	56.1	7.2
◇	23	.762	1.753		223	191	219	358		30.5	26.3	.37	.43	.135	.865	56.9	9.6
◊	24	1.270	2.286		204	172	204	118	5.8	39.6	33.8	.48	.56	.148	.852	64.7	8.6
▴	25	1.270	2.311		191	159	191	246	5.8	37.0	31.0	.44	.52	.159	.841	60.6	8.7
▾	26	1.270	2.540		161	130	158	983	5.8	30.7	24.9	.35	.43	.191	.809	54.7	7.0
◻	27	2.54	3.556		128	95.9	125	30	10.2	42.5	32.2	.45	.60	.241	.759	58.5	12.8
◇	28	2.54	3.708		96.6	64.9	96.6	492	10.2	31.7	21.4	.30	.45	.323	.677	----	9.9
▽	29	2.54	4.216		88.3	56.6	88.3	1613	10.2	28.9	18.6	.26	.41	.355	.645	47.0	11.1

TABLE IV. - INITIAL CONDITIONS AND TEST DATA AT -423° F (20° K)

(a) U. S. customary units

Symbol	Specimen number	$2a_i$, in.	$2a_L$, in.	σ_{min} , ksi	σ_{max} , ksi	$\Delta\sigma$, ksi	σ_F , ksi	N_F , cycles to failure	$K_{min,i}$, ksi $\sqrt{\text{in.}}$	$K_{max,i}$, ksi $\sqrt{\text{in.}}$	ΔK_i , ksi $\sqrt{\text{in.}}$	$\Delta K_i/K_c$	$K_{max,i}/K_c$	R_i	$\Delta K_i/K_{max,i}$	$K_{max,L}$, ksi $\sqrt{\text{in.}}$	γ
Tensile																	
□	30	0.128	0.60	6.0	56.0	50.0	56.0	280	2.7	28.8	26.1	0.47	0.52	0.093	0.907	64.8	6.8
□	31	.301	.91	4.4	41.4	37.0	40.5	277	3.0	30.7	27.6	.50	.56	.099	.901	56.5	8.8
□	32	.496	1.53	3.0	29.3	26.3	29.3	911	2.6	27.1	24.5	.44	.49	.097	.903	55.7	8.0
□	33	.996	1.84	4.0	22.5	18.5	21.6	753	5.3	30.4	25.1	.46	.55	.174	.826	50.1	9.3
Tank																	
■	34	0.125	0.33	5.5	54.6	49.1	48.4	278	2.6	28.6	26.0	0.47	0.52	0.090	0.909	52.3	6.7
■	35	.300	.63	3.7	36.6	32.9	-----	272	2.9	30.5	27.6	.50	.55	.095	.905	51.6	7.1
■	36	.500	.99	2.4	23.8	21.4	23.3	401	2.6	27.1	24.5	.44	.49	.097	.903	46.3	9.5
■	37	1.000	1.71	2.8	15.8	14.4	-----	415	5.3	30.4	25.1	.46	.55	.174	.826	49.7	10.6

(b) SI units

Symbol	Specimen number	$2a_i$, in.	$2a_L$, in.	σ_{min} , MN/m ²	σ_{max} , MN/m ²	$\Delta\sigma$, MN/m ²	σ_F , MN/m ²	N_F , cycles to failure	$K_{min,i}$, MN/m ^{3/2}	$K_{max,i}$, MN/m ^{3/2}	ΔK_i , MN/m ^{3/2}	$\Delta K_i/K_c$	$K_{max,i}/K_c$	R_i	$\Delta K_i/K_{max,i}$	$K_{max,L}$, MN/m ^{3/2}	γ
Tensile																	
□	30	0.325	1.524	41.4	386	345	386	280	3.0	31.7	28.7	0.47	0.52	0.093	0.907	71.3	6.8
□	31	.765	2.311	30.4	286	255	279	277	3.3	33.8	30.4	.50	.56	.099	.901	62.2	8.8
□	32	1.260	3.886	20.7	202	181	202	911	2.9	29.8	27.0	.44	.49	.097	.903	60.6	8.0
□	33	2.530	4.674	27.6	155	128	149	753	5.8	33.4	27.6	.46	.55	.174	.826	55.1	9.3
Tank																	
■	34	0.318	0.838	38.0	377	339	334	278	2.9	31.5	28.6	0.47	0.52	0.090	0.909	57.5	6.7
■	35	.762	1.600	25.5	253	277	-----	272	3.2	33.6	30.4	.50	.55	.095	.905	56.8	7.1
■	36	1.270	2.515	16.6	164	148	161	401	2.9	29.8	27.0	.44	.49	.097	.903	50.9	9.5
■	37	2.540	4.343	19.3	109	99.4	-----	415	5.8	33.4	27.6	.46	.55	.174	.826	54.7	10.6

TABLE V. - CRACK GROWTH DATA FOR TENSILE TESTS AT -320°F (77°K)

(a) U. S. customary units

Symbol	Specimen number	2a, in.	N, cycles	K_{\max}' ksi $\sqrt{\text{in.}}$	K_{\min}' ksi $\sqrt{\text{in.}}$	ΔK , ksi $\sqrt{\text{in.}}$	Symbol	Specimen number	2a, in.	N, cycles	K_{\max}' ksi $\sqrt{\text{in.}}$	K_{\min}' ksi $\sqrt{\text{in.}}$	ΔK , ksi $\sqrt{\text{in.}}$	Symbol	Specimen number	2a, in.	N, cycles	K_{\max}' ksi $\sqrt{\text{in.}}$	K_{\min}' ksi $\sqrt{\text{in.}}$	ΔK , ksi $\sqrt{\text{in.}}$
○	1	0.126	0	30.4	2.1	28.3	◻	6	0.300	0	34.1	3.2	30.9	◻	11	0.496	0	28.0	4.1	23.9
		.192	50	32.2	2.2	30.1			.319	20	35.2	3.3	31.9			.532	200	29.1	4.3	24.8
		.167	100	35.0	2.4	32.6			.341	40	36.4	3.4	33.0			.579	400	30.5	4.5	26.0
		.210	150	39.3	2.7	36.7			.367	60	37.8	3.5	34.3			.634	600	32.0	4.7	27.3
		.232	170	41.4	2.8	38.7			.401	80	39.6	3.7	36.0			.702	800	33.9	5.0	28.9
		.272	190	44.9	3.0	41.9			.450	100	42.2	3.9	38.2			.778	1000	35.9	5.2	30.7
		.303	200	47.6	3.2	44.4			.488	110	44.0	4.1	40.0			.892	1200	39.0	5.7	33.3
		.358	210	51.9	3.5	48.5			.551	120	47.1	4.3	42.7			.999	1300	41.8	6.1	35.8
		.425	213	57.0	3.8	53.2			.678	130	53.0	4.9	48.1			1.197	1400	47.4	6.8	40.6
		.590	215	69.0	4.5	64.4			.820	133	59.5	5.4	54.1			1.640	1447	63.2	8.6	54.6
◻	2	0.126	0	28.1	2.0	26.1	◻	7	0.296	0	30.0	3.2	26.8	◻	12	1.001	0	38.9	6.1	32.8
		.131	40	28.6	2.1	26.6			.327	50	31.6	3.3	28.2			1.073	20	40.7	6.3	34.4
		.139	80	29.5	2.1	27.4			.361	100	33.2	3.5	29.7			1.126	40	42.1	6.5	35.5
		.150	120	30.7	2.2	28.4			.400	150	35.1	3.7	31.4			1.171	60	43.2	6.7	36.5
		.170	160	32.7	2.4	30.3			.449	200	37.3	3.9	33.4			1.221	80	44.6	6.9	37.7
		.203	200	35.8	2.6	33.2			.531	250	40.8	4.3	36.5			1.284	100	46.4	7.1	39.3
		.258	240	40.4	2.9	37.5			.600	270	43.6	4.5	39.1			1.336	110	47.7	7.3	40.4
		.308	260	44.3	3.2	41.1			.667	280	46.3	4.8	41.5			1.407	120	49.9	7.6	42.3
		.425	275	52.6	3.8	48.8			.800	290	51.6	5.3	46.2			1.610	130	56.8	8.5	48.3
		.560	277	61.4	4.4	57.1			.920	293	56.4	5.8	50.6			1.670	131	59.2	8.7	50.5

◇	3	0.128	0	27.1	2.1	25.1	◇	8	0.300	0	27.8	3.2	24.6	△	13	0.999	0	34.2	6.1	28.1
		.137	100	28.1	2.1	26.0			.321	100	28.8	3.3	25.5			1.033	30	34.9	6.2	28.7
		.149	200	29.3	2.2	27.1			.345	200	29.9	3.4	26.4			1.100	100	35.7	6.3	29.3
		.163	300	30.7	2.3	28.3			.376	300	31.2	3.6	27.7			1.100	150	36.4	6.4	30.0
		.179	400	32.2	2.4	29.7			.429	400	33.4	3.8	29.6			1.134	200	37.2	6.6	30.6
		.202	500	34.2	2.6	31.6			.476	450	35.3	4.0	31.3			1.172	250	38.0	6.7	31.3
		.247	600	37.9	2.9	35.0			.561	500	38.6	4.4	34.2			1.232	300	39.4	6.9	32.4
		.315	700	47.1	3.6	43.5			.639	525	41.5	4.7	36.8			1.329	350	41.7	7.3	34.4
		.550	743	58.2	4.3	53.8			.795	550	47.1	5.3	41.8			1.493	388	45.9	8.0	38.0
		.840	751	76.1	5.5	70.6			1.000	560	54.5	6.1	48.5			1.790	400	55.8	9.3	46.5
△	4	0.128	0	24.1	2.1	22.0	◇	9	0.496	0	36.1	4.1	32.0	◇	14	0.942	0	28.8	6.0	22.8
		.138	200	25.0	2.1	22.8			.542	20	37.9	4.3	33.6			1.039	200	29.7	6.2	23.5
		.150	400	26.0	2.2	23.8			.583	40	39.4	4.5	35.0			1.083	400	30.7	6.4	24.3
		.168	600	27.6	2.4	25.2			.628	60	41.1	4.7	36.4			1.159	600	31.9	6.6	25.2
		.201	800	30.2	2.6	27.6			.694	80	43.5	4.9	38.6			1.254	800	33.7	7.0	26.7
		.223	900	31.8	2.7	29.1			.738	90	45.0	5.1	40.0			1.325	900	35.1	7.3	27.8
		.257	1000	34.2	2.9	31.3			.797	100	47.2	5.3	41.9			1.437	1000	37.4	7.7	29.6
		.323	1100	38.5	3.3	35.2			.914	110	51.4	5.7	45.6			1.560	1050	40.1	8.2	31.9
		.470	1150	47.0	4.0	43.0			1.000	113	54.5	6.1	48.5			1.705	1080	43.8	8.9	34.9
		.940	1163	71.8	5.8	65.9			1.130	116	59.6	6.5	53.0			1.820	1088	47.2	9.5	37.7
△	5	0.301	0	36.9	3.2	33.7	◇	10	0.495	0	33.8	4.1	29.7	▽	15	0.995	0	26.3	6.0	20.3
		.327	10	38.5	3.3	35.2			.519	20	34.6	4.2	30.4			1.042	400	27.1	6.2	20.9
		.355	20	40.2	3.5	36.8			.547	40	35.6	4.3	31.3			1.105	800	28.1	6.4	21.7
		.388	30	42.1	3.6	38.5			.573	60	36.5	4.4	32.1			1.211	1200	29.9	6.8	23.1
		.423	40	44.1	3.8	40.4			.600	80	37.5	4.5	32.9			1.282	1400	31.1	7.1	24.0
		.470	50	46.7	4.0	42.7			.630	100	38.5	4.7	33.8			1.393	1600	33.1	7.5	25.6
		.530	60	49.9	4.3	45.6			.678	120	40.1	4.9	35.3			1.594	1800	37.1	8.4	28.8
		.572	65	52.1	4.4	47.7			.744	140	42.3	5.1	37.2			1.695	1830	39.4	8.9	30.6
		.640	69	55.6	4.7	50.9			.858	160	46.1	5.5	40.5			1.945	1900	46.5	10.2	36.3
		.740	70	60.7	5.1	55.6			1.190	174	57.6	6.8	50.9			2.170	1906	57.1	11.7	45.4

TABLE V. - Concluded. CRACK GROWTH DATA FOR TENSILE TESTS AT -320° F (77° K)

(b) SI units

Symbol	Specimen number	2a, cm	N, cycles	K_{max}' MN/m ^{3/2}	K_{min}' MN/m ^{3/2}	ΔK , MN/m ^{3/2}	Symbol	Specimen number	2a, cm	N, cycles	K_{max}' MN/m ^{3/2}	K_{min}' MN/m ^{3/2}	ΔK , MN/m ^{3/2}	Symbol	Specimen number	2a, cm	N, cycles	K_{max}' MN/m ^{3/2}	K_{min}' MN/m ^{3/2}	ΔK , MN/m ^{3/2}
○	1	0.320	0	33.4	2.3	31.1	D	6	0.762	0	37.5	3.5	34.0	D	11	1.260	0	30.8	4.5	26.3
		.361	50	35.4	2.4	33.1			.810	20	38.7	3.6	35.1			1.351	200	32.0	4.7	27.3
		.424	100	38.5	2.6	35.9			.866	40	40.0	3.7	36.3			1.471	400	33.6	5.0	28.6
		.533	150	43.2	3.0	40.4			.932	60	41.6	3.8	37.7			1.610	600	35.2	5.2	30.0
		.589	170	45.5	3.1	42.6			1.019	80	43.6	4.1	39.6			1.783	800	37.3	5.5	31.8
		.691	190	49.4	3.3	46.1			1.143	100	46.4	4.3	42.0			1.976	1000	39.5	5.7	33.8
		.770	200	52.4	3.5	48.8			1.240	110	48.4	4.5	44.0			2.266	1200	42.9	6.3	36.6
		.909	210	57.1	3.8	53.4			1.400	120	51.8	4.7	47.0			2.537	1300	46.0	6.7	39.4
		1.080	213	62.7	4.2	58.5			1.722	130	58.3	5.4	52.9			3.040	1400	52.1	7.5	44.7
		1.499	215	75.9	5.0	70.8			2.083	133	65.4	5.9	59.5			4.166	1447	69.5	9.5	60.1
□	2	0.320	0	30.9	2.2	28.7	□	7	0.752	0	33.0	3.5	29.5	▷	12	2.543	0	42.8	6.7	36.1
		.333	40	31.5	2.3	29.3			.831	50	34.8	3.6	31.0			2.725	20	44.8	6.9	37.8
		.353	80	32.4	2.3	30.1			.917	100	36.5	3.8	32.7			2.860	40	46.3	7.2	39.0
		.381	120	33.8	2.4	31.2			1.016	150	38.6	4.1	34.5			2.974	60	47.5	7.4	40.2
		.432	160	36.0	2.6	33.3			1.140	200	41.0	4.3	36.7			3.101	80	49.1	7.6	41.5
		.516	200	39.4	2.9	36.5			1.349	250	44.9	4.7	40.2			3.274	100	51.0	7.8	43.2
		.655	240	44.4	3.2	41.2			1.524	270	48.0	5.0	43.0			3.393	110	52.5	8.0	44.4
		.782	260	48.7	3.5	45.2			1.694	280	50.9	5.3	45.6			3.574	120	54.9	8.4	46.5
		1.080	275	57.9	4.2	53.7			2.032	290	56.8	5.8	50.8			4.089	130	62.5	9.4	53.1
		1.422	277	67.5	4.8	62.8			2.337	293	62.0	6.4	55.7			4.242	131	65.1	9.6	55.6

◇	3	0.325	0	29.8	2.3	27.6	◇	8	0.762	0	30.6	3.5	27.1	△	13	2.537	0	37.6	6.7	30.9
		.348	100	30.9	2.3	28.6			.815	100	31.7	3.6	28.0			2.624	50	38.4	6.8	31.6
		.378	200	32.2	2.4	29.8			.876	200	32.9	3.7	29.0			2.708	100	39.3	6.9	32.2
		.414	300	33.8	2.5	31.1			.955	300	34.3	4.0	30.5			2.794	150	40.0	7.0	33.0
		.455	400	35.4	2.6	32.7			1.090	400	36.7	4.2	32.6			2.880	200	40.9	7.3	33.7
		.513	500	37.6	2.9	34.8			1.209	450	38.8	4.4	34.4			2.977	250	41.8	7.4	34.4
		.627	600	41.7	3.2	38.5			1.425	500	37.6	4.8	37.6			3.129	300	43.3	7.6	35.6
		.952	700	51.8	4.0	47.8			1.623	525	45.6	5.2	40.5			3.376	350	45.9	8.0	37.8
		1.397	743	64.0	4.7	59.2			2.019	550	51.8	5.8	46.0			3.792	388	50.5	8.8	41.8
		2.134	751	83.7	6.0	77.7			2.540	560	60.0	6.7	53.4			4.547	400	61.4	10.2	51.2
△	4	0.325	0	26.5	2.3	24.2	◇	9	1.260	0	39.7	4.5	35.2	◇	14	2.520	0	31.7	6.6	25.1
		.351	200	27.5	2.3	25.1			1.377	20	41.7	4.7	37.0			2.639	200	32.7	6.8	25.8
		.381	400	28.6	2.4	26.2			1.481	40	43.3	5.0	38.5			2.776	400	33.8	7.0	26.7
		.427	600	30.4	2.6	27.7			1.595	60	45.2	5.2	40.0			2.944	600	35.1	7.3	27.7
		.511	800	33.2	2.9	30.4			1.763	80	47.8	5.4	42.5			3.185	800	37.1	7.7	29.4
		.566	900	35.0	3.0	32.0			1.875	90	49.5	5.6	44.0			3.366	900	38.6	8.0	30.6
		.653	1000	37.6	3.2	34.4			2.024	100	51.9	5.8	46.1			3.650	1000	41.1	8.5	32.6
		.820	1100	42.4	3.6	38.7			2.322	110	56.5	6.3	50.2			3.962	1050	44.1	9.0	35.1
		1.194	1150	51.7	4.4	47.3			2.540	113	60.0	6.7	53.4			4.331	1080	48.2	9.8	38.4
		2.388	1163	79.0	6.4	72.5			2.870	116	65.6	7.2	58.3			4.623	1088	51.9	10.4	41.5
▷	5	0.765	0	40.6	3.5	37.1	△	10	1.257	0	37.2	4.5	32.7	▽	15	2.527	0	28.9	6.6	22.3
		.831	10	42.4	3.6	38.7			1.318	20	38.1	4.6	33.4			2.647	400	29.8	6.8	23.0
		.902	20	44.2	3.8	40.5			1.389	40	39.2	4.7	34.4			2.807	800	30.9	7.0	23.9
		.986	30	46.3	4.0	42.4			1.455	60	40.2	4.8	35.3			3.076	1200	32.9	7.5	25.4
		1.074	40	48.5	4.2	44.4			1.524	80	41.2	5.0	36.2			3.256	1400	34.2	7.8	26.4
		1.194	50	51.4	4.4	47.0			1.600	100	37.2	5.2	37.2			3.538	1600	36.4	8.2	28.2
		1.346	60	54.9	4.7	50.2			1.722	120	44.1	5.4	38.8			4.049	1800	40.8	9.2	31.7
		1.453	65	57.3	4.8	52.5			1.890	140	46.5	5.6	40.9			4.305	1850	43.3	9.8	33.7
		1.626	69	61.2	5.2	56.0			2.179	160	50.7	6.0	44.6			4.940	1900	51.2	11.2	39.9
		1.880	70	66.8	5.6	61.2			3.023	174	63.4	7.5	56.0			5.512	1906	62.8	12.9	49.9

TABLE VI. - CRACK GROWTH DATA FOR TANK TESTS AT -320° F (77° K)

(a) U. S. customary units

Symbol	Specimen number	2a, in.	N, cycles	K _{max} ', ksi√in.	K _{min} ', ksi√in.	ΔK, ksi√in.	Symbol	Specimen number	2a, in.	N, cycles	K _{max} ', ksi√in.	K _{min} ', ksi√in.	ΔK, ksi√in.	Symbol	Specimen number	2a, in.	N, cycles	K _{max} ', ksi√in.	K _{min} ', ksi√in.	ΔK, ksi√in.
●	16	0.125	0	30.0	2.2	27.8	■	21	0.300	0	33.8	3.7	30.1	●	26	0.500	0	27.9	5.3	22.6
		.143	40	32.5	2.4	30.1			.326	20	35.9	4.0	31.9			.521	200	28.8	5.5	23.3
		.165	80	35.5	2.6	32.9			.356	40	38.2	4.2	34.0			.558	400	30.4	5.8	24.6
		.192	120	39.1	2.8	36.2			.398	60	41.3	4.5	36.8			.618	600	32.9	6.3	26.6
		.210	140	41.4	3.0	38.4			.417	65	42.6	4.7	38.1			.667	700	35.0	6.6	28.4
		.246	160	46.0	3.3	42.7			.494	70	44.8	4.4	39.9			.732	800	37.8	7.2	30.7
		.264	165	48.3	3.4	44.8			.496	75	48.8	5.3	43.5			.770	850	39.4	7.5	32.0
		.287	170	51.2	3.6	47.5			.539	77.5	52.1	5.6	46.5			.808	900	41.1	7.8	33.3
		.330	175	56.6	4.0	52.6			.620	80	52.2	6.3	52.2			.863	950	43.5	8.2	35.3
		.504	180	79.3	5.4	74.0			.680	81	63.3	6.7	56.5			1.000	983	49.7	9.3	40.4
■	17	0.125	0	27.8	2.2	25.6	■	22	0.300	0	30.1	3.7	26.3	■	27	1.000	0	38.6	9.3	29.3
		.142	100	30.0	2.4	27.7			.316	40	31.2	3.9	27.3			1.074	3	41.2	9.9	31.3
		.166	200	33.1	2.6	30.5			.338	80	32.7	4.1	28.6			1.112	7	42.5	10.2	32.3
		.184	250	35.3	2.8	32.5			.364	120	34.4	4.3	30.1			1.131	10	43.2	10.4	32.8
		.214	300	38.8	3.0	35.8			.384	140	35.7	4.4	31.3			1.147	13	43.8	10.5	33.3
		.239	320	41.7	3.2	38.5			.421	160	38.2	4.7	33.5			1.168	17	44.6	10.7	33.8
		.259	330	44.0	3.4	40.6			.453	170	40.3	5.0	35.4			1.187	20	45.2	10.9	34.4
		.283	340	46.8	3.6	43.2			.506	180	43.9	5.4	38.5			1.215	23	46.3	11.1	35.2
		.326	350	51.8	4.0	47.8			.545	185	46.5	5.7	40.8			1.282	27	48.7	11.7	37.0
		.520	356	74.7	5.5	69.2			.610	191	51.0	6.2	44.8			1.400	30	53.2	12.7	40.5

◆	18	0.125	0	26.7	2.2	24.5	◆	23	0.300	0	27.7	3.7	23.9	◆	28	1.000	0	28.8	9.3	19.5
		.136	100	28.1	2.3	25.8			.318	100	28.7	3.9	24.9			1.042	100	29.9	9.7	20.2
		.149	200	29.7	2.4	27.2			.356	200	31.1	4.2	26.9			1.073	200	30.7	9.9	20.8
		.166	300	31.7	2.6	29.1			.383	250	32.8	4.4	28.3			1.127	300	32.1	10.4	21.7
		.191	400	34.6	2.8	31.8			.424	300	35.3	4.7	30.5			1.170	350	33.2	10.7	22.5
		.213	450	37.1	3.0	34.1			.452	320	37.0	5.0	32.0			1.242	400	35.2	11.3	23.8
		.249	500	41.1	3.3	37.8			.498	340	39.8	5.3	34.5			1.294	425	36.6	11.8	24.8
		.295	540	46.2	3.7	42.5			.541	350	42.4	5.7	36.8			-----	-----	-----	-----	-----
		.370	570	54.4	4.3	50.1			.595	356	45.7	6.1	39.7			-----	-----	-----	-----	-----
		.480	584	66.7	5.2	61.5			.690	358	51.7	6.8	44.9			-----	-----	-----	-----	-----
▲	19	0.125	0	23.6	2.2	21.4	◆	24	0.500	0	36.0	5.3	30.7	▼	29	1.000	0	26.3	9.3	16.9
		.135	200	24.7	2.3	22.4			.558	40	39.2	5.8	33.4			1.023	400	26.8	9.5	17.4
		.150	400	26.3	2.4	23.9			.625	80	42.9	6.3	36.6			1.084	800	28.3	10.0	18.2
		.170	600	28.4	2.6	25.8			.636	85	43.5	6.4	37.1			1.162	1200	30.1	10.7	19.4
		.201	800	31.6	2.9	28.6			.649	90	44.3	6.5	37.8			1.192	1300	30.8	10.9	19.9
		.222	900	33.7	3.1	30.6			.665	95	45.2	6.6	38.5			1.232	1400	31.8	11.3	20.6
		.250	1000	36.3	3.3	33.0			.684	100	46.2	6.8	39.5			1.301	1500	33.5	11.8	21.7
		.294	1100	40.6	3.7	36.9			.711	105	47.8	7.0	40.8			1.370	1550	35.2	12.4	22.8
		.352	1150	46.1	4.2	41.9			.751	110	50.1	7.3	42.8			1.510	1600	38.8	13.7	25.1
		.530	1176	63.1	5.6	57.6			.900	118	58.8	8.5	50.3			1.620	1613	41.6	14.7	27.0
▲	20	0.300	0	36.5	3.7	32.8	▲	25	0.500	0	33.6	5.3	28.2							
		.328	10	38.9	4.0	34.9			.547	100	36.0	5.7	30.3							
		.358	20	41.4	4.2	37.1			.577	140	37.5	5.9	31.6							
		.390	30	44.0	4.5	39.5			.623	180	39.9	6.3	33.6							
		.424	40	46.8	4.7	42.1			.658	200	41.6	6.6	35.1							
		.446	45	48.7	4.9	43.8			.678	210	42.7	6.7	36.0							
		.474	50	51.0	5.1	45.9			.705	220	44.1	6.9	37.2							
		.519	55	54.8	5.5	49.3			.746	230	46.3	7.3	39.0							
		.556	57.5	57.9	5.8	52.2			.814	240	49.9	7.8	42.1							
		.594	59	61.2	6.1	55.1			.910	246	55.1	8.6	46.6							

TABLE VI. - Concluded. CRACK GROWTH DATA FOR TENSILE TESTS AT -320° F (77° K)

(b) SI units

Symbol	Specimen number	2a, cm	N, cycles	K _{max} , MN/m ^{3/2}	K _{min} , MN/m ^{3/2}	ΔK, MN/m ^{3/2}	Symbol	Specimen number	2a, cm	N, cycles	K _{max} , MN/m ^{3/2}	K _{min} , MN/m ^{3/2}	ΔK, MN/m ^{3/2}	Symbol	Specimen number	2a, cm	N, cycles	K _{max} , MN/m ^{3/2}	K _{min} , MN/m ^{3/2}	ΔK, MN/m ^{3/2}
●	16	0.318	0	33.0	2.4	30.6	■	21	0.762	0	37.2	4.1	33.1	■	26	1.270	0	30.7	5.8	24.9
		.363	40	35.8	2.6	33.1			.828	20	39.5	4.4	35.1			1.323	200	39.5	6.0	25.6
		.419	80	39.0	2.9	36.2			.904	40	42.0	4.6	37.4			1.417	400	33.4	6.4	27.1
		.488	120	43.0	3.1	39.8			1.011	60	45.4	5.0	40.5			1.570	600	36.2	6.9	29.3
		.533	140	45.5	3.3	42.2			1.059	65	47.1	5.2	41.9			1.694	700	38.5	7.3	31.2
		.625	160	50.6	3.6	47.8			1.128	70	49.3	5.4	43.9			1.859	800	41.6	7.9	33.8
		.671	165	53.1	3.7	49.3			1.260	75	53.7	5.8	47.8			1.956	850	43.3	8.2	35.2
		.729	170	56.3	4.0	52.2			1.369	77.5	57.3	6.2	51.2			2.052	900	45.2	8.6	36.6
		.838	175	62.3	4.4	57.9			1.575	80	64.4	6.9	57.4			2.192	950	47.8	9.0	38.8
		1.280	180	87.2	5.9	81.4			1.727	81	69.6	7.4	62.2			2.540	983	54.7	10.2	44.4
■	17	0.318	0	30.6	2.4	28.2	■	22	0.762	0	33.1	4.1	28.9	●	27	2.540	0	42.5	10.2	32.2
		.361	100	33.0	2.6	30.5			.803	40	34.3	4.3	30.0			2.728	3	45.3	10.9	34.4
		.422	200	36.4	2.9	33.6			.859	80	36.0	4.5	31.5			2.824	7	46.8	11.2	35.5
		.467	250	38.8	3.1	35.8			.925	120	37.8	4.7	33.1			2.873	10	47.5	11.4	36.1
		.544	300	42.7	3.3	39.4			.975	140	39.3	4.8	34.4			2.913	13	48.2	11.6	36.6
		.607	320	45.9	3.5	42.4			1.069	160	42.0	5.2	36.8			2.767	17	49.1	11.8	37.2
		.658	330	48.4	3.7	44.7			1.151	170	44.3	5.5	38.9			3.015	20	49.7	12.0	37.8
		.719	340	51.5	4.0	47.5			1.285	180	48.3	5.9	42.4			3.086	23	50.9	12.2	38.7
		.828	350	57.0	4.4	52.6			1.384	185	51.2	6.3	44.9			3.256	27	53.6	12.9	40.7
		1.321	356	82.2	6.0	76.1			1.549	191	56.1	6.8	49.3			3.556	30	58.5	14.0	44.6

●	18	0.318	0	29.4	2.4	27.0	●	23	0.762	0	30.5	4.1	26.3	●	28	2.540	0	31.7	10.2	21.4
		.345	100	30.9	2.5	28.4			.808	100	31.6	4.3	27.4			2.647	100	32.9	10.7	22.2
		.378	200	32.7	2.6	29.9			.904	200	34.2	4.6	29.6			2.725	200	33.8	10.9	22.9
		.422	300	34.9	2.9	32.0			.973	250	36.1	4.8	31.1			2.863	300	35.3	11.4	23.9
		.485	400	38.1	3.1	35.0			1.077	300	38.8	5.2	33.6			2.972	350	36.5	11.8	24.8
		.541	450	40.8	3.3	37.5			1.148	320	40.7	5.5	35.2			3.155	400	38.7	12.4	26.2
		.632	500	45.2	3.6	41.6			1.265	340	43.8	5.8	38.0			3.287	425	40.3	13.0	27.3
		.749	540	50.8	4.1	46.8			1.374	350	46.6	6.3	40.5			-----	---	----	----	----
		.940	570	59.8	4.7	55.1			1.511	356	50.3	6.7	43.7			-----	---	----	----	----
		1.219	584	73.4	5.7	67.6			1.753	358	56.9	7.5	49.4			-----	---	----	----	----
▲	19	0.318	0	26.0	2.4	23.5	◆	24	1.270	0	39.6	5.8	33.8	▼	29	2.540	0	28.9	10.2	18.6
		.343	200	27.2	2.5	24.6			1.417	40	43.1	6.9	36.7			2.598	400	29.5	10.4	19.0
		.381	400	28.9	2.6	26.3			1.588	80	47.2	6.9	40.3			2.753	800	31.1	11.0	20.0
		.432	600	31.2	2.9	28.4			1.615	85	47.8	7.0	40.8			2.951	1200	33.1	11.8	21.3
		.511	800	34.8	3.2	31.5			1.648	90	48.7	7.2	41.6			3.028	1300	33.9	12.0	21.9
		.564	900	37.1	3.4	33.7			1.689	95	49.7	7.3	42.4			3.129	1400	35.0	12.4	22.7
		.635	1000	39.9	3.6	36.3			1.737	100	50.8	7.5	43.4			3.305	1500	36.8	13.0	23.9
		.747	1100	44.7	4.1	40.6			1.806	105	52.6	7.7	44.9			3.480	1550	38.7	13.6	25.1
		.894	1150	50.7	4.6	46.1			1.908	110	55.1	8.0	47.1			3.835	1600	42.7	15.1	27.6
		1.346	1176	69.4	6.2	63.4			2.286	118	64.7	9.4	55.3			4.115	1613	45.8	16.2	29.7
▲	20	0.762	0	40.2	4.1	36.1	▲	25	1.270	0	37.0	5.8	31.0							
		.833	10	42.8	4.4	38.4			1.389	100	39.6	6.3	33.3							
		.909	20	45.5	4.6	40.3			1.466	140	41.2	6.5	34.8							
		.991	30	48.4	5.0	43.4			1.582	180	43.9	6.9	37.0							
		1.077	40	51.5	5.2	46.3			1.659	200	45.8	7.3	38.6							
		1.133	45	53.6	5.4	48.2			1.722	210	47.0	7.4	39.6							
		1.204	50	56.1	5.6	50.5			1.791	220	48.5	7.6	40.9							
		1.318	55	60.3	6.0	54.2			1.895	230	50.9	8.0	42.9							
		1.412	59.5	63.7	6.4	57.4			2.068	240	54.9	8.6	46.3							
		1.509	59	67.3	6.7	60.6			2.311	246	60.6	9.5	51.3							

TABLE VII. - CRACK GROWTH DATA FOR TENSILE AND TANK TESTS AT -423° F (20° K)

(a) U. S. customary units

Symbol	Specimen number	2a, in.	N, cycles	K_{max}' ksi√in.	K_{min}' ksi√in.	ΔK , ksi√in.	Symbol	Specimen number	2a, in.	N, cycles	K_{max}' ksi√in.	K_{min}' ksi√in.	ΔK , ksi√in.
Tensile													
Q	30	0.128	0	28.8	2.7	26.1	Q	32	0.496	0	27.1	2.6	24.5
		.138	40	29.9	2.8	27.1			.549	200	28.6	2.8	25.9
		.149	80	31.1	2.9	28.2			.606	400	30.2	2.9	27.3
		.162	120	32.4	3.0	29.4			.643	500	31.2	3.0	28.2
		.181	160	34.3	3.2	31.1			.694	600	32.6	3.2	29.4
		.209	200	36.9	3.4	33.5			.768	700	34.5	3.3	31.1
		.230	220	38.8	3.6	35.2			.887	800	37.5	3.6	33.9
		.262	240	41.4	3.8	37.6			.984	850	40.0	3.9	36.1
		.326	260	46.4	4.3	42.1			1.210	900	46.0	4.4	41.6
		.600	280	64.8	5.9	58.9			1.530	911	55.8	5.2	50.5
◇	31	0.301	0	30.7	3.0	27.6	◇	33	0.996	0	30.4	5.3	25.1
		.310	40	31.1	3.1	28.1			1.034	100	31.1	5.4	25.7
		.331	80	32.2	3.2	29.0			1.079	200	32.0	5.5	26.4
		.368	120	34.0	3.4	30.7			1.126	300	32.9	5.7	27.2
		.410	160	36.0	3.6	32.4			1.179	400	33.9	5.9	28.0
		.461	200	38.3	3.8	34.5			1.246	500	35.2	6.1	29.1
		.490	220	39.6	3.9	35.7			1.338	600	37.1	6.4	30.7
		.533	240	41.4	4.1	37.3			1.487	700	40.4	6.9	33.4
		.617	260	44.9	4.4	40.5			1.583	730	42.7	7.3	35.4
		.910	277	56.5	5.5	51.0			1.840	753	50.1	8.4	41.7
Tank													
●	34	0.125	0	28.6	2.6	26.0	●	36	0.500	0	27.2	2.6	24.5
		.132	50	29.6	2.7	26.9			.528	100	28.2	2.8	25.5
		.142	100	30.8	2.8	28.0			.562	200	29.5	2.9	26.7
		.156	150	32.5	2.9	29.6			.582	250	30.3	3.0	27.4
		.180	200	35.4	3.2	32.2			.607	300	31.3	3.0	28.2
		.194	220	37.1	3.3	33.7			.628	325	32.1	3.1	29.0
		.211	240	39.1	3.5	35.6			.665	350	33.5	3.3	30.3
		.236	260	42.0	3.8	38.3			.738	375	36.4	3.5	32.8
		.259	270	44.5	4.0	40.6			.808	388	39.1	3.8	35.3
		.330	278	52.3	4.6	47.7			.990	401	46.3	4.5	41.9
◆	35	0.300	0	30.5	2.9	27.6	◆	37	1.000	0	30.4	5.3	25.1
		.318	50	31.7	3.0	28.7			1.136	250	33.9	5.9	28.0
		.338	100	33.0	3.1	29.9			1.172	300	34.9	6.0	28.8
		.362	150	34.6	3.3	31.3			1.197	325	35.5	6.2	29.3
		.401	200	37.1	3.5	33.6			1.230	350	36.4	6.3	30.1
		.425	220	38.6	3.6	35.0			1.282	375	37.8	6.5	31.2
		.461	240	40.9	3.8	37.0			1.385	400	40.6	7.0	33.5
		.536	260	45.6	4.3	41.4			1.435	405	41.9	7.2	34.7
		.607	270	50.1	4.7	45.5			1.510	410	44.0	7.6	36.4
		.630	272	51.6	4.8	46.8			1.710	415	49.7	8.6	41.1

TABLE VII. - Concluded. CRACK GROWTH DATA FOR TENSILE AND TANK TESTS AT -423° F (20° K)

(b) SI units

Symbol	Specimen number	2a, cm	N, cycles	K_{max}' MN/m ^{3/2}	K_{min}' MN/m ^{3/2}	ΔK MN/m ^{3/2}	Symbol	Specimen number	2a, cm	N, cycles	K_{max}' MN/m ^{3/2}	K_{min}' MN/m ^{3/2}	ΔK MN/m ^{3/2}
Tensile													
Q	30	0.325	0	31.7	3.0	28.7	Q	32	1.260	0	29.8	2.9	27.0
		.351	40	32.9	3.1	29.8			1.394	200	31.5	3.1	28.5
		.378	80	34.2	3.2	31.0			1.539	400	33.2	3.2	30.0
		.411	120	35.6	3.3	32.3			1.633	500	34.3	3.3	31.0
		.460	160	37.7	3.5	34.2			1.763	600	35.9	3.5	32.3
		.531	200	40.6	3.7	36.8			1.951	700	38.0	3.6	34.2
		.584	220	42.7	4.0	38.7			2.253	800	41.2	4.0	37.3
		.655	240	45.5	4.2	41.4			2.499	850	44.0	4.3	39.7
		.828	260	51.0	4.7	46.3			3.073	900	50.6	4.8	45.8
		1.524	280	71.3	6.5	64.8			3.886	911	61.4	5.7	55.6
Q	31	0.765	0	33.8	3.3	30.4	Q	33	2.530	0	33.4	5.8	27.6
		.787	40	34.2	3.4	30.9			2.626	100	34.2	5.9	28.3
		.841	80	35.4	3.5	31.9			2.741	200	35.2	6.0	29.0
		.935	120	37.4	3.7	33.8			2.860	300	36.2	6.3	29.9
		1.041	160	39.6	4.0	35.6			2.995	400	37.3	6.5	30.8
		1.171	200	42.1	4.2	38.0			3.165	500	38.7	6.7	32.0
		1.245	220	43.6	4.3	39.3			3.399	600	40.8	7.0	33.8
		1.354	240	45.5	4.5	41.0			3.777	700	44.4	7.6	36.7
		1.567	260	49.4	4.8	44.6			4.021	730	47.0	8.0	38.9
		2.311	277	62.2	6.0	56.1			4.674	753	55.1	9.2	45.9
Tank													
Q	34	0.318	0	31.5	2.9	28.6	Q	36	1.270	0	29.9	2.9	27.0
		.335	50	32.6	3.0	39.6			1.341	100	31.0	3.1	28.0
		.361	100	33.9	3.1	30.8			1.427	200	32.4	3.2	29.4
		.396	150	35.8	3.2	32.6			1.478	250	33.3	3.3	30.1
		.457	200	38.9	3.5	35.4			1.542	300	34.4	3.3	31.0
		.493	220	40.8	3.6	37.1			1.595	325	35.3	3.4	31.9
		.536	240	43.0	3.8	39.2			1.689	350	36.8	3.6	33.3
		.599	260	46.2	4.2	42.1			1.875	375	40.0	3.8	36.1
		.658	270	49.0	4.4	44.7			2.052	388	43.0	4.2	38.8
		.838	278	57.5	5.1	52.5			2.515	401	50.9	5.0	46.1
Q	35	0.762	0	33.6	3.2	30.4	Q	37	2.540	0	33.4	5.8	27.6
		.808	50	34.9	3.3	31.6			2.885	250	37.3	6.5	30.8
		.859	100	36.3	3.4	32.9			2.977	300	38.4	6.6	31.7
		.919	150	38.1	3.6	34.4			3.040	325	39.0	6.8	32.2
		1.019	200	40.8	3.8	37.0			3.124	350	40.0	6.9	33.1
		1.080	220	42.5	4.0	38.5			3.256	375	41.6	7.2	34.3
		1.171	240	45.0	4.2	40.7			3.518	400	44.7	7.7	36.8
		1.361	260	50.2	4.7	45.5			3.645	405	46.1	7.9	38.2
		1.542	270	55.1	5.2	50.0			3.835	410	48.4	8.4	40.0
		1.600	272	56.8	5.3	51.5			4.343	415	54.7	9.5	45.2

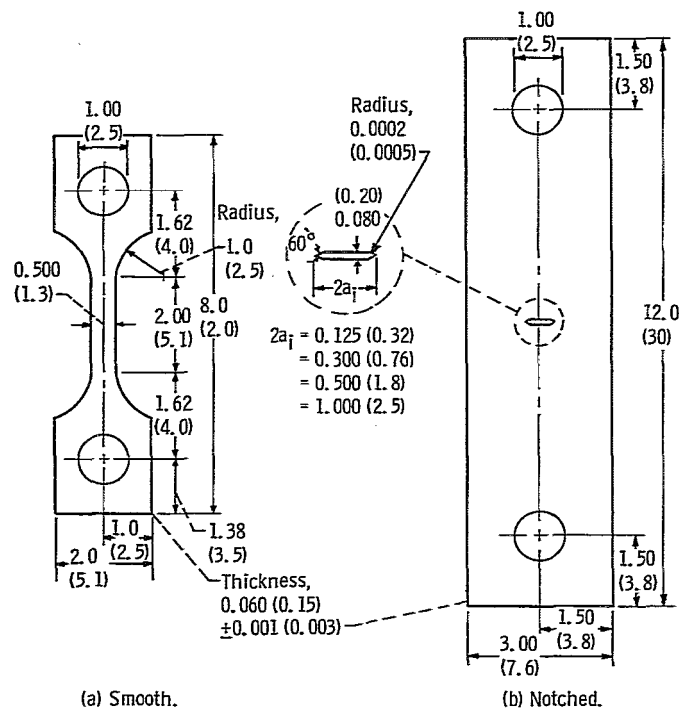


Figure 1. - Smooth and notched tensile specimens. (Dimensions are in inches (cm)).

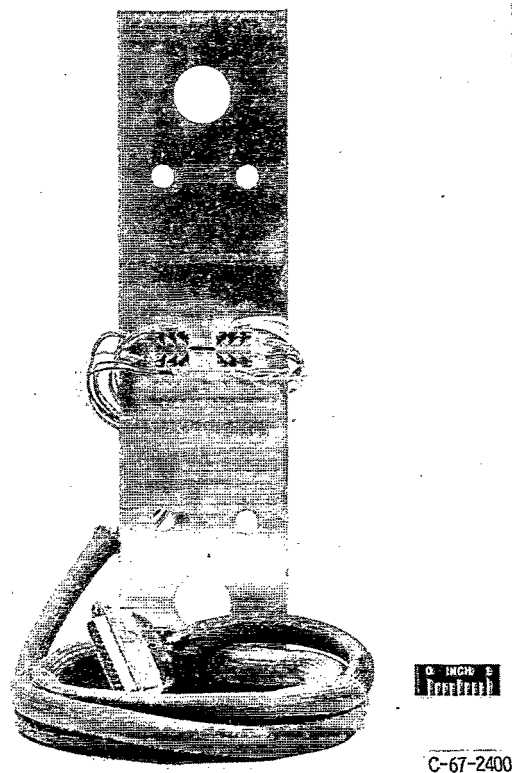


Figure 2. - Notched tensile specimen with continuity gages.

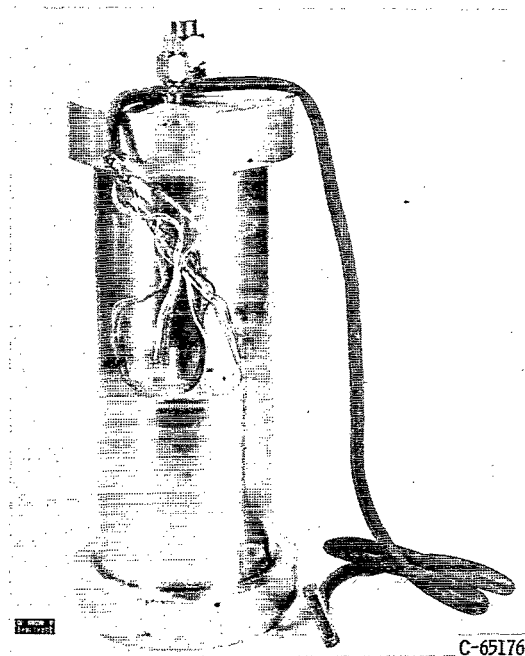


Figure 3. - Notched tank test specimen with continuity gages.

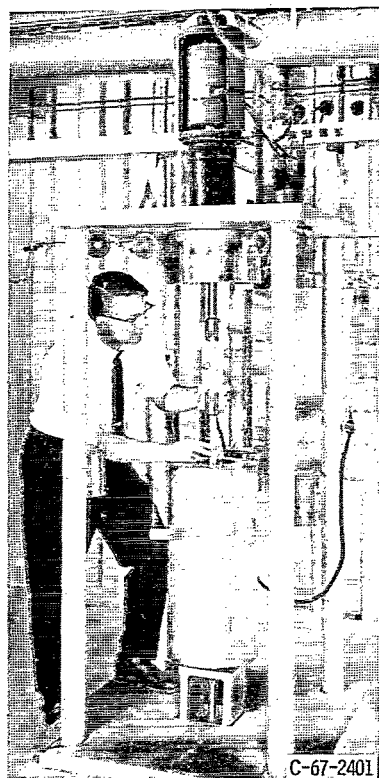


Figure 4. - Tensile fatigue testing machine.

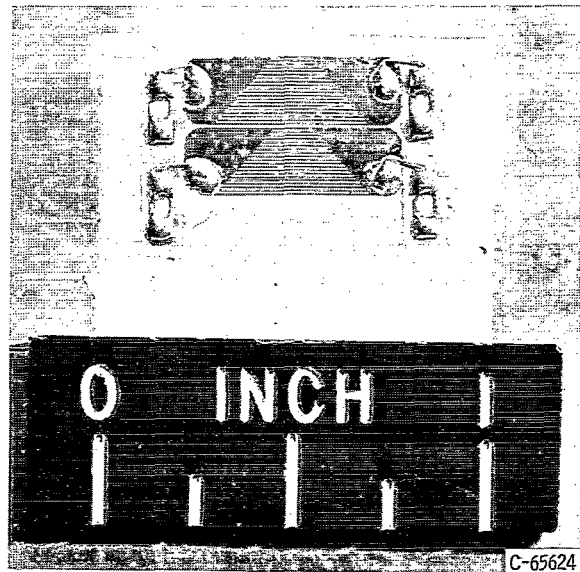


Figure 5. - Two continuity gages mounted in tandem at notch tip.

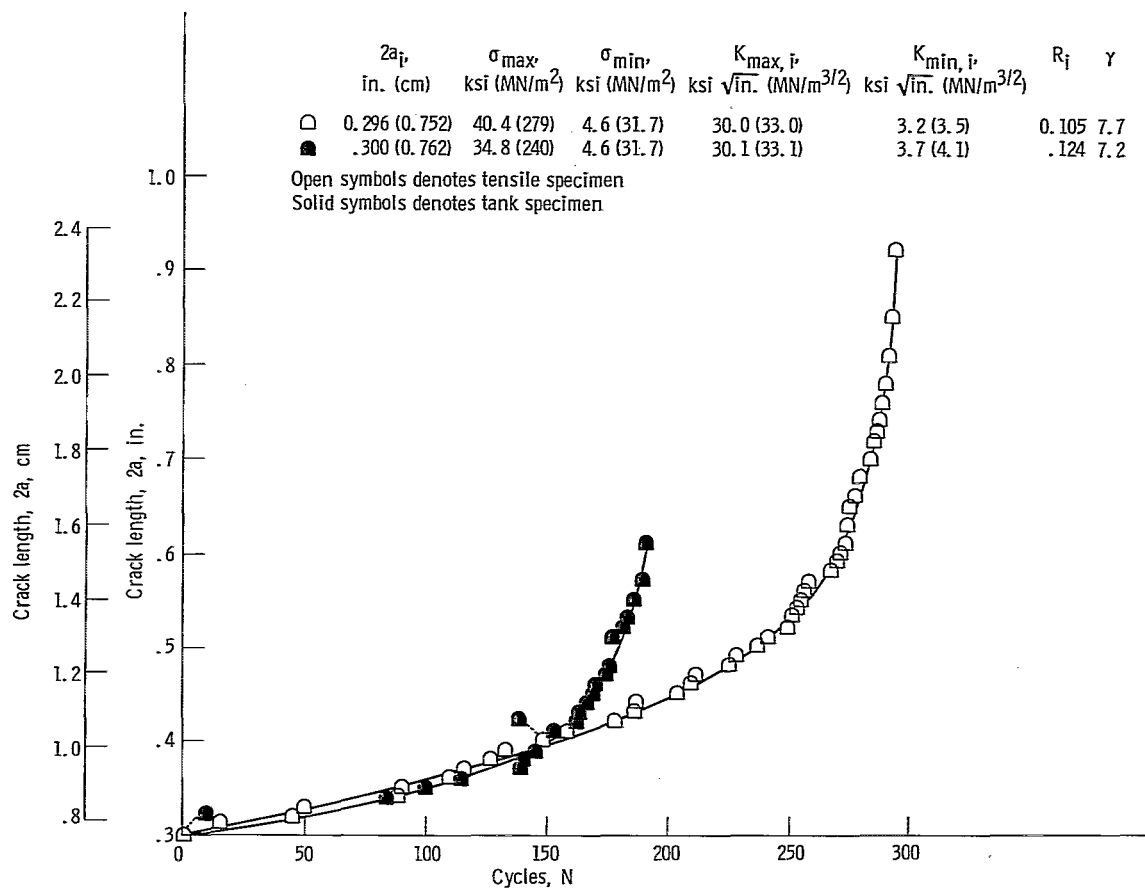


Figure 6. - Typical curve of crack growth as function of stress cycles at -320° F.

Specimen number	$2a_i$, in. (cm)	σ_{max} , ksi (MN/m ²)	σ_{min} , ksi (MN/m ²)	$K_{max, i}$, ksi $\sqrt{\text{in.}}$ (MN/m ^{3/2})	$K_{min, i}$, ksi $\sqrt{\text{in.}}$ (MN/m ^{3/2})	R_i	γ	N
○ 1	0.126 (0.320)	57.3 (395)	4.6 (31.7)	30.4 (33.4)	2.1 (2.3)	0.068	7.3	215
● 16	.125 (.318)	54.9 (379)		30.0 (33.0)	2.2 (2.4)	.073	6.0	180
□ 2	.126 (.320)	54.2 (374)		28.1 (30.9)	2.0 (2.2)	.073	7.6	277
■ 17	.125 (.318)	51.8 (357)		27.8 (30.6)	2.2 (2.4)	.079	6.2	356
◇ 3	.128 (.325)	52.5 (362)		27.1 (29.8)	2.1 (2.3)	.076	6.7	751
● 18	.125 (.318)	50.1 (346)		26.7 (29.4)	2.2 (2.4)	.082	5.6	584
△ 4	.128 (.325)	47.8 (330)		24.1 (26.5)	2.1 (2.3)	.086	6.3	1163
▲ 19	.125 (.318)	45.4 (313)		23.6 (26.0)	2.2 (2.4)	.093	6.0	1176

— — Tensile specimens.
 — Tank specimens

Open symbols denote tensile specimens
 Solid symbols denote tank specimens

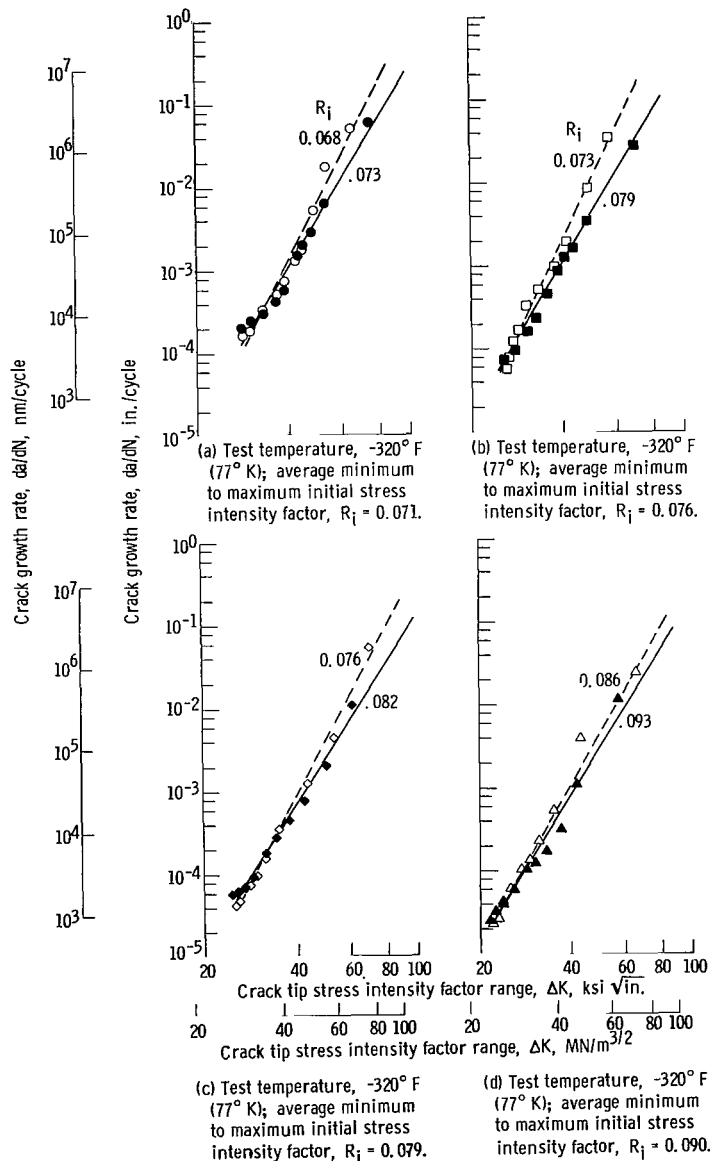


Figure 7. - Crack growth rate as function of crack tip stress intensity factor range for tensile and tank specimens.

Specimen number	$2a_i$, in. (cm)	σ_{max} , ksi (MN/m ²)	σ_{min} , ksi (MN/m ²)	$K_{max, i}$, ksi $\sqrt{\text{in.}}$ (MN/m ^{3/2})	$K_{min, i}$, ksi $\sqrt{\text{in.}}$ (MN/m ^{3/2})	R_i	γ	N	
△	5	0.301 (0.764)	47.6 (328)	4.6 (31.7)	36.9 (40.6)	3.2 (3.5)	0.086	9.8	70
▲	20	.300 (.762)	41.2 (284)	↓	36.5 (40.2)	3.7 (4.1)	.102	7.1	59
▮	6	.300 (.762)	44.7 (308)		34.1 (37.5)	3.2 (3.5)	.093	7.9	133
▮	21	.300 (.762)	38.6 (266)		33.8 (37.2)	3.7 (4.1)	.111	7.6	81
□	7	.296 (.752)	40.4 (279)		30.0 (33.0)	3.2 (3.5)	.105	7.7	293
■	22	.300 (.762)	34.8 (240)		30.1 (33.1)	3.7 (4.1)	.124	7.2	191
○	8	.300 (.762)	37.6 (259)		27.8 (30.6)	3.2 (3.5)	.114	7.8	560
●	23	.300 (.762)	32.3 (223)		27.7 (30.5)	3.7 (4.1)	.135	9.6	358

— — — Tensile specimens
———— Tank specimens

Open symbols denote tensile specimens
Solid symbols denote tank specimens

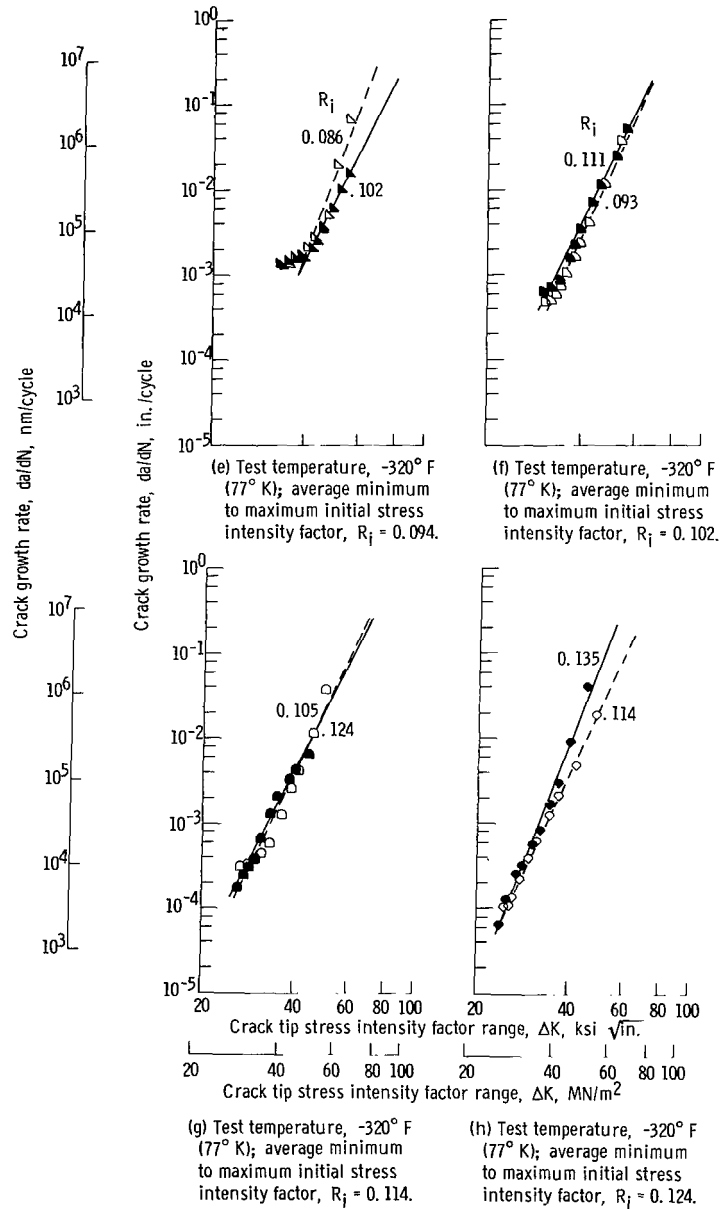


Figure 7. - Continued.

Specimen number	$2a_i$, in. (cm)	σ_{max} , ksi (MN/m ²)	σ_{min} , ksi (MN/m ²)	$K_{max, i}$, ksi $\sqrt{\text{in.}}$ (MN/m ^{3/2})	$K_{min, i}$, ksi $\sqrt{\text{in.}}$ (MN/m ^{3/2})	R_i	γ	N
◇ 9	0.496 (1.260)	37.6 (259)	4.6 (31.7)	36.1 (39.7)	4.1 (4.5)	0.114	8.8	116
◆ 24	.500 (1.270)	29.5 (204)		36.0 (39.6)	5.3 (5.8)	.148	8.6	118
△ 10	.495 (1.257)	35.5 (245)		33.8 (37.2)	4.1 (4.5)	.122	8.3	174
▲ 25	.500 (1.270)	37.7 (191)		33.6 (37.0)	5.3 (5.8)	.159	8.7	246
□ 11	.496 (1.260)	30.0 (207)		28.0 (30.8)	4.1 (4.5)	.147	6.5	1447
● 26	.500 (1.270)	23.4 (161)		27.9 (30.7)	5.3 (5.8)	.191	7.0	983

— — — Tensile specimens
— Tank specimens

Open symbols denote tensile specimens
Solid symbols denote tank specimens

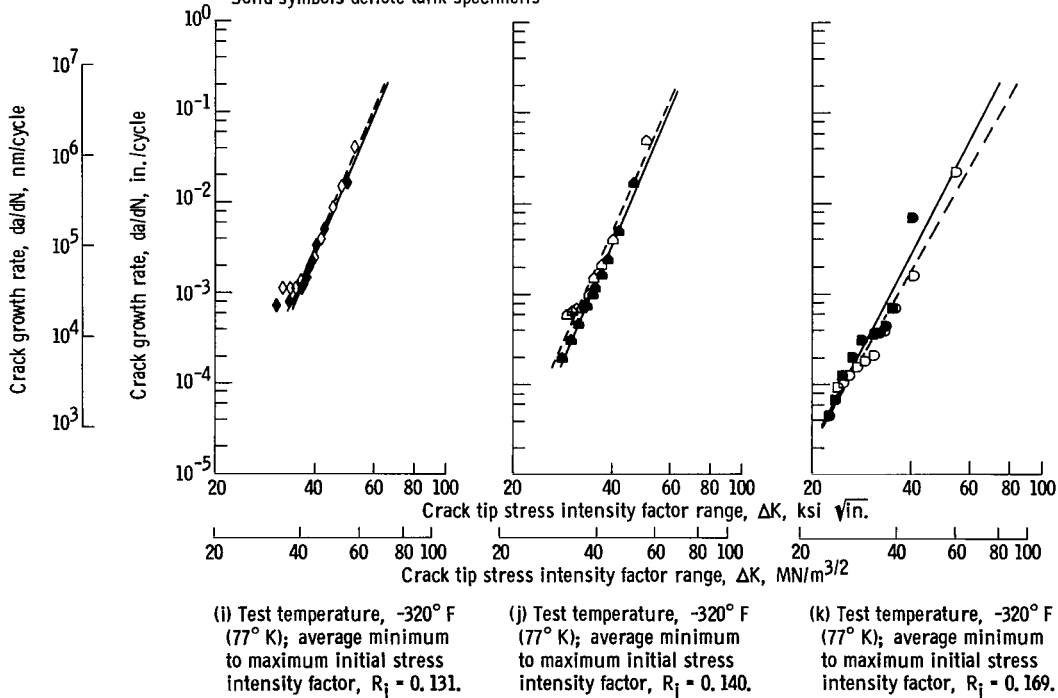


Figure 7. - Continued.

Specimen number	$2a_i$, in. (cm)	σ_{max} , ksi (MN/m ²)	σ_{min} , ksi (MN/m ²)	$K_{max,i}$, ksi $\sqrt{\text{in.}}$ (MN/m ^{3/2})	$K_{min,i}$, ksi $\sqrt{\text{in.}}$ (MN/m ^{3/2})	R_i	γ	N
◇ 12	1.001 (2.543)	28.1 (194)	4.6 (31.7)	38.9 (42.8)	6.1 (6.7)	0.156	11.2	131
● 27	1.000 (2.54)	18.5 (128)		38.6 (42.5)	9.3 (10.2)	.241	12.8	30
△ 13	.999 (2.537)	25.0 (172)		34.2 (37.6)	6.1 (6.7)	.177	11.1	400
○ 14	0.992 (2.520)	21.4 (148)		28.8 (31.7)	6.0 (6.6)	.209	8.9	1088
● 28	1.000 (2.54)	14.0 (96.6)		28.8 (31.7)	9.3 (10.2)	.323	9.9	492
▽ 15	.995 (2.572)	19.6 (135)		26.3 (28.9)	6.0 (6.6)	.230	7.9	1906
▼ 29	1.000 (2.54)	12.8 (88.3)		26.3 (28.9)	9.3 (10.2)	.355	11.1	1613

--- Tensile specimens
 — Tank specimens

Open symbols denote tensile specimens
 Solid symbols denote tank specimens

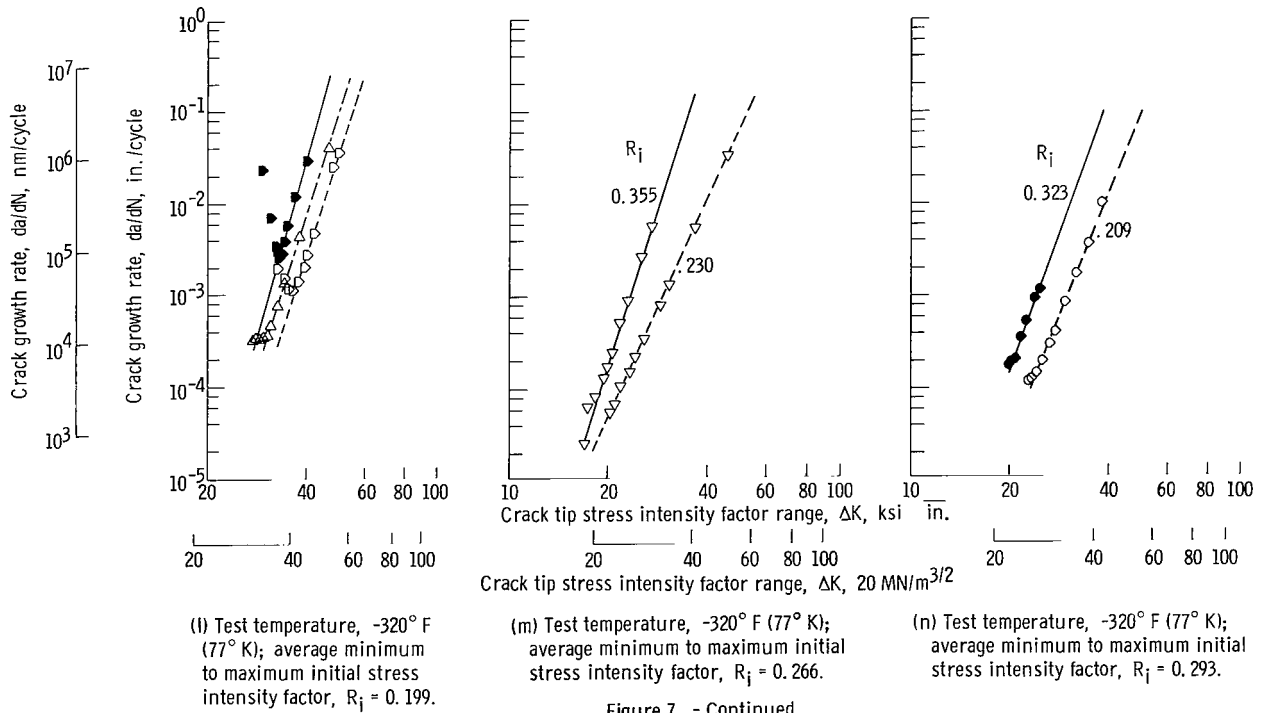


Figure 7. - Continued.

Specimen number	$2a_i$, in. (cm)	σ_{max} , ksi (MN/m ²)	σ_{min} , ksi (MN/m ²)	$K_{max, i}$, ksi $\sqrt{in.}$ (MN/m ^{3/2})	$K_{min, i}$, ksi $\sqrt{in.}$ (MN/m ^{3/2})	R_i	γ	N
30	0.125 (0.325)	56.0 (386)	6.0 (41.4)	28.8 (31.7)	2.7 (3.0)	0.093	6.8	280
34	.125 (.318)	54.6 (377)	5.5 (38.0)	28.6 (31.5)	2.6 (2.9)	.093	6.7	278
31	.301 (.765)	41.4 (286)	4.0 (30.4)	30.7 (33.8)	3.0 (3.3)	.099	8.8	277
35	.300 (.762)	36.6 (253)	3.7 (25.5)	30.5 (33.6)	2.9 (3.2)	.095	7.1	272
32	.496 (1.260)	29.3 (202)	3.0 (20.7)	27.1 (29.8)	2.6 (2.9)	.097	8.0	911
36	.500 (1.270)	23.8 (164)	2.4 (16.6)	27.1 (29.8)	2.6 (2.9)	.097	9.5	401
33	.996 (2.530)	22.5 (155)	4.0 (27.6)	30.4 (33.4)	5.3 (5.8)	.174	9.3	753
37	1.000 (2.540)	15.8 (109)	2.8 (19.3)	30.4 (33.4)	5.3 (5.8)	.174	10.6	415

--- Tensile specimens
 — Tank specimens

Open symbols denote tensile specimens
 Solid symbols denote tank specimens

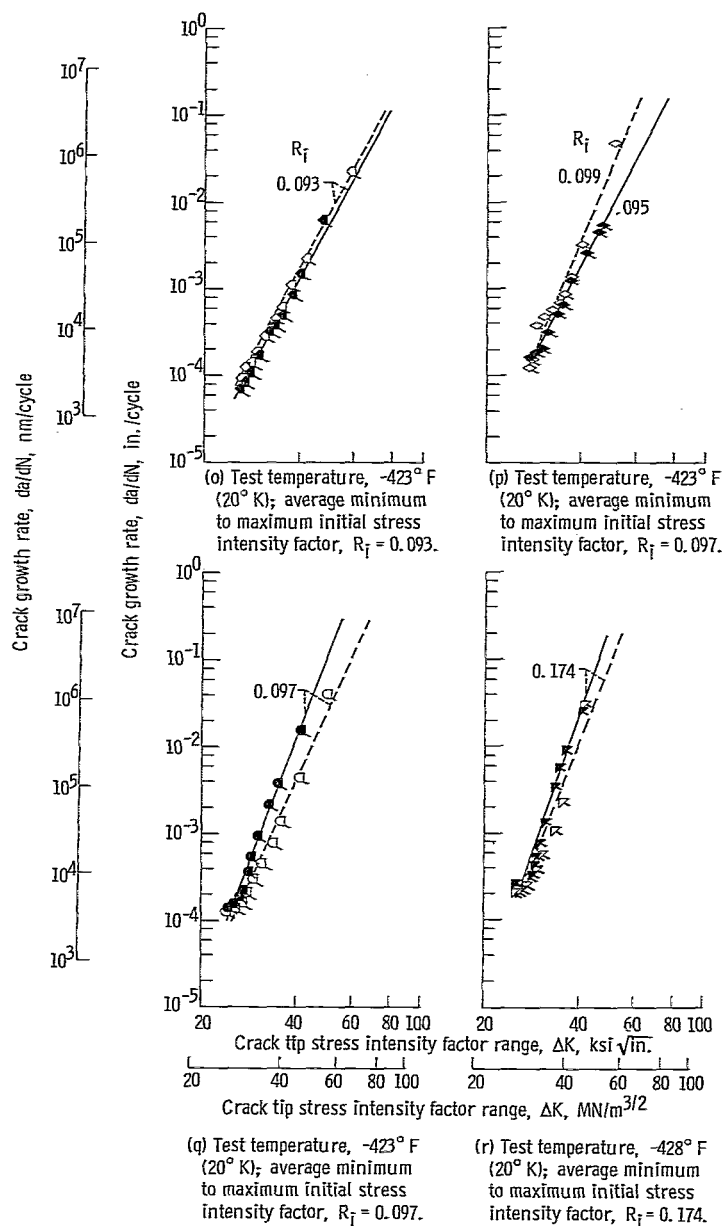


Figure 7. - Concluded.

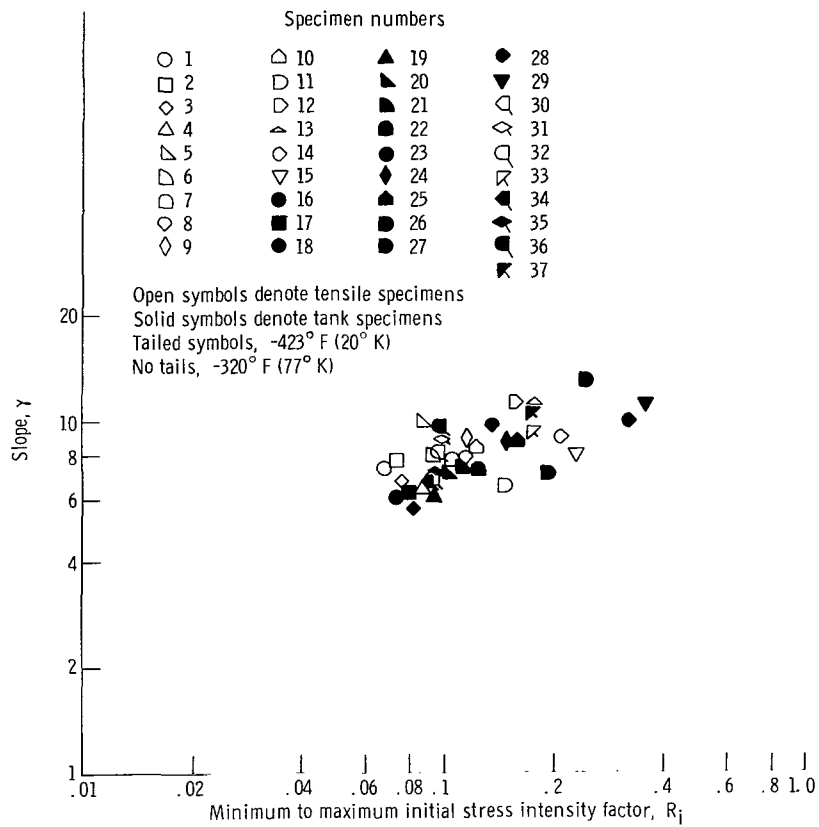


Figure 8. - Relation of minimum to maximum initial stress intensity factor to slope.

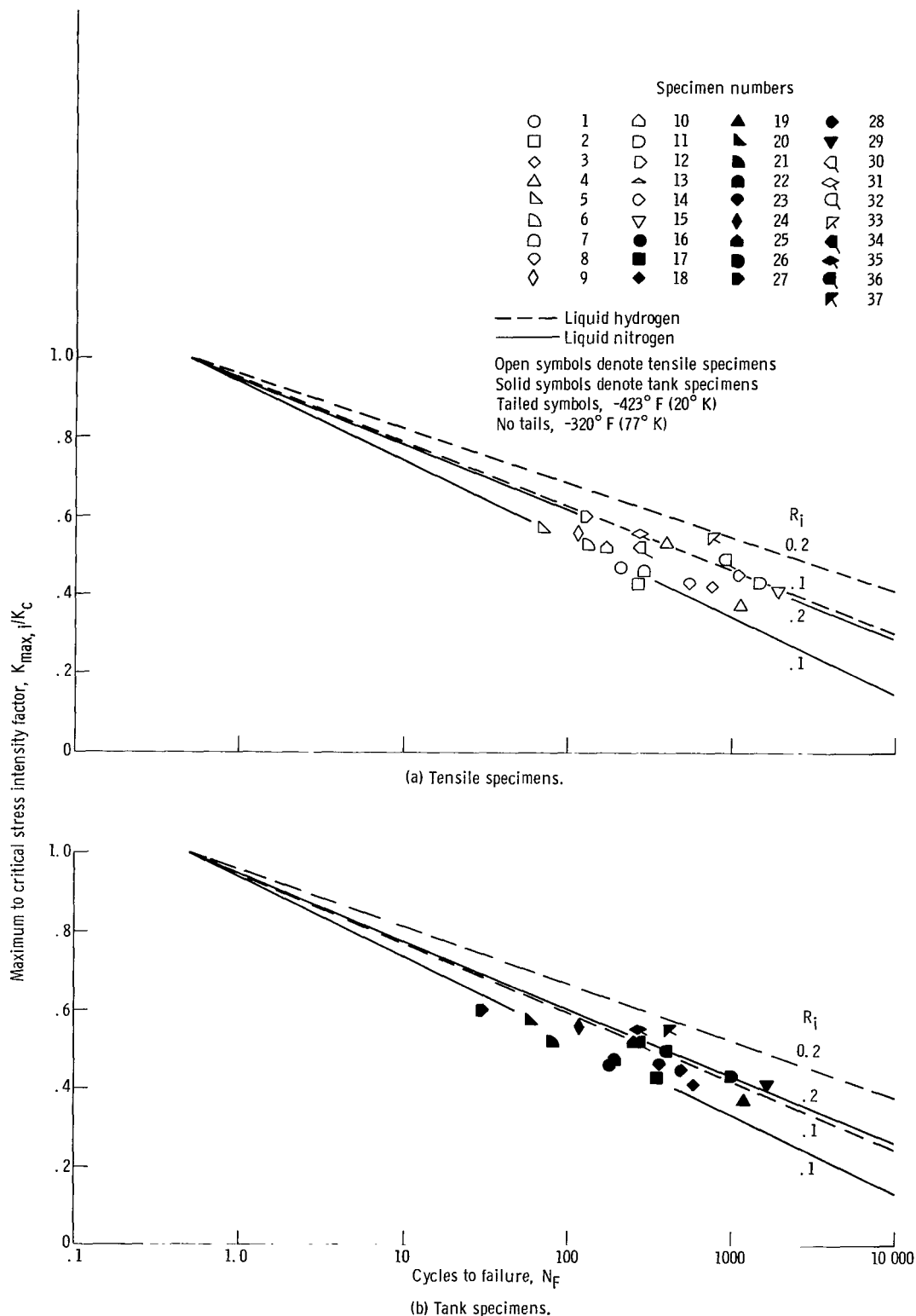


Figure 9. - Effect of $K_{\max, i}/K_C$ and R_i ratio on cycles to failure. (See tables II and III for test conditions.)

Washington, D.C. 20546